4 H_2 permeation through Pd films

4.1 Introduction

It is of great importance to understand the fundamentals of H_2 permeation through a freestanding Pd film (or foil) before studying the H_2 permeation through composite Pd membranes. The H_2 permeation mechanism through thin Pd films involves: the dissociation of H_2 to H atoms at the surface of the Pd film, the diffusion of the H atoms across the Pd layer and the recombination of H atoms into H_2 at the opposite surface. Such a diffusion mechanism is denoted as "solution-diffusion" mechanism since H_2 permeates through Pd by forming a PdH alloy. Each of the above-described steps could be the rate-limiting step for H_2 permeation through the Pd foil. The activation energy for H_2 desorption is given by Equation (4-1).

$$E_d = E_a - \Delta_r H \tag{4-1}$$

where E_d and E_a are the activation energy for H_2 desorption and H_2 absorption respectively. $\Delta_r H$ is the heat of the H_2 absorption reaction. The dissociative absorption of H_2 is a slightly activated process, therefore, $E_d \approx -\Delta_r H$ and at low temperatures, the associative desorption of H_2 is the rate-limiting step for H_2 permeation. The Temperature Programmed Desorption (TPD) of H_2 from Pd/γ-Al_2O_3 showed three desorption peaks (Ragaini et al., 1994). The first desorption peak was attributed to the H dissolved in the bulk and the activation energy for H desorption was found to be 50.2 kJ mol^{-1}. The two

other peaks corresponded to a weakly chemisorbed H specie and a strongly bound H specie respectively. The activation energy for the weakly and the strongly bound H species was 85.7 and 92-133 kJ mol^{-1} respectively (Ragaini et al., 1994). The temperature at which the desorption peak of the strongly bound H specie occurs was found to be equal to 150ºC (Kurman et al., 1990; Ragaini et al., 1994) and 77ºC (Farias et al., 1997). Hence at temperatures higher than 150ºC, when both absorption/desorption are at the thermodynamic equilibrium ($r_{absorption}=r_{desorption}$), the H diffusion through the bulk of Pd is the rate-limiting step for hydrogen permeation. However, if the Pd film thickness is very small, the diffusion of H atoms across the Pd film is very fast and the H_2 desorption becomes the rate-limiting step even though both absorption/desorption are at the thermodynamic equilibrium. The model for the H_2 permeation through Pd foils developed by Ward and Dao, (1999), proved that for a Pd foil with a clean surface, the H diffusion through the Pd bulk was the rate-limiting step at temperatures higher than 300ºC even for membranes with thicknesses approaching 1μm. They also proved that the desorption of H_2 is the rate-limiting step at low temperatures and that absorption is the rate-limiting step only at very low H_2 partial pressures (<<1 bar) or in the case of severe surface contamination.

When the diffusion of H atoms through the Pd bulk is the rate limiting step, Fick's first law is assumed, and the H_2 flux permeating through the Pd foil is proportional to the difference in the amount of H dissolved at the high pressure side of the membrane and the amount of H dissolved at the low pressure side of the membrane. In order to determine the concentration of H dissolved in the Pd, a relation between H_2 pressure in the gas phase and the H dissolved in the Pd bulk needs to be used. At very low H_2 pressures, the

relation between H_2 pressure and H dissolved in the Pd, n(H/Pd), is given by Equation (4-2) (Sieverts et al., 1915).

$$P_{H_2}^{0.5} = K(T) \cdot n(H/Pd) \qquad (4\text{-}2)$$

where P_{H2} is the H_2 pressure, K(T) is a proportionality constant named as Sieverts' constant and n(H/Pd) is the H concentration in the Pd bulk. Therefore, at low H_2 pressures, the H_2 flux, J_{H2}, is proportional to ($P^{0.5}{}_1$- $P^{0.5}{}_2$), with P_1 the high H_2 pressure and P_2 the low H_2 pressure. Since Equation (4-2) is only valid at low pressures, deviations from Sieverts' law (the H_2 pressure exponent ≠0.5) can occur at high H_2 pressures. For instance, at 250ºC, the H_2 absorption isothermal ($P^{0.5}$, *n(H/Pd)*) is linear at low pressures, 0–ca. 0.5 bar but starts to curve as the miscibility gap is approached, i.e. P_{H2} > 1 bar (Gillespie and Galstaun, 1936). Therefore, in the 1.1-2 bar pressure range, the H_2 flux, J_{H2}, is proportional to ($P^{\text{n-exponent}}{}_1$- $P^{\text{n-exponent}}{}_2$) with n-exponent >0.5. The permeation of H_2 through thick Pd foils (100 μm) was studied by Morreale et al. (2003) at very high pressures, and the n-exponents were calculated based on permeation data from four pressure ranges (1.01-1.75, 1.01-7.75, 1.0-16.00, 1.01-26.00 bar). They reported an increase in the n-exponent from 0.53 (the limit value) to 0.65 as the pressure range was increased. Unfortunately, Morreale et al. (2003) did not report the temperature at which the reported n-exponents vs. pressure range were determined and it would be difficult to compare their experimental values with other reported values. Deviations from Sieverts' law also occur in thin Pd foils when the Pd foil is defective and allows for the passage of other gases and when the surface of the Pd foil has low activity for the dissociation of H_2, which happens when contaminants are adsorbed on the surface.

In this chapter, the fundamentals of H_2 absorption in Pd are described. The equation relating H_2 pressure and temperature with H_2 dissolved in Pd is established and the equation of H_2 permeation through Pd is derived. The influence of leakages and low catalytic activity of the surface on the permeation mechanism of H_2 properties are described in Chapter 5.

4.2 Results and discussion

4.2.1 H_2 concentration in Pd: n(H/Pd)

The concentration of H_2 in Pd is usually denoted as "n" and has the units of mol H/mol Pd. The H_2 concentration in Pd, "n", was denoted as n(H/Pd) in this entire thesis. This section aimed at understanding and establishing the relation between P_{H2} and n(H/Pd) for the α phase at temperatures between 250 and 500ºC. The Pd-H phase diagram, inset in Figure 2-1, shows linear absorption isotherms ($P^{0.5}$ as a function of H loading, n(H/Pd)) in a narrow range of pressure for a given temperature. Figure 4-1 shows the absorption isotherms, $P^{0.5}{}_{H2}$ as a function of n(H/Pd), at 250, 290 and 310ºC reported by Gillespie and Galstaun (1936). For the three isotherms pictured in Figure 4-1 and for H_2 pressures higher than 5 bar (=2.23 $bar^{0.5}$), the relation $P^{0.5}$ as a function of H_2 loading, n(H/Pd), is not linear and Equation (4-2) is not valid. The relation between $P^{0.5}{}_{H2}$ and n(H/Pd) is better described by Equation (4-3)

$$P_{H_2}^{n-\exp onent} = K'(T) \cdot n(H/Pd) \qquad (4\text{-}3)$$

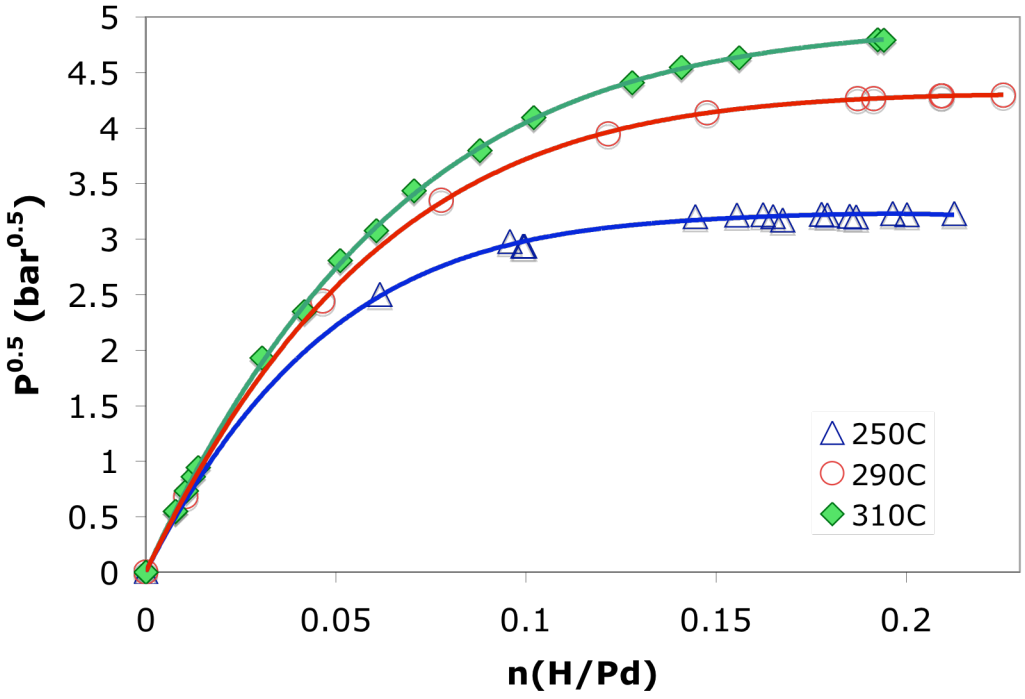

Figure 4-1 $P^{0.5}$ vs. n(H/Pd) data from Gillespie and Galstaun (1936). The experimental data were fitted with a 4^{th} order polynomial function (solid lines)

The H_2 partial pressure exponent is usually called "n" or "n-value" in the literature, yet, in this thesis the H_2 partial pressure exponent will be denoted as n-exponent in order not to confuse it with the H content, n(H/Pd). The experimental data reported by Gillespie and Galstaun (1936) were used to calculate the n-exponent as a function of pressure for the 250, 290 and 310ºC isotherms in Figure 4-1. The n-exponents were calculated by first plotting the raw data (P_{H2} vs. n(H/Pd) of the original publication) in the ($P^{0.5}{}_{H2}$, n(H/Pd)) form for the three isotherms as shown in Figure 4-1. For each isotherm, the ($P^{0.5}{}_{H2}$ vs. n(H/Pd)) experimental points were fitted with a 4^{th} order polynomial function also seen in Figure 4-1.

The 4^{th} order polynomial function was used for the interpolation of the experimental data points between 0 and 0.1 n(H/Pd) at a step of 0.005 n(H/Pd). In order to determine the n-exponent as a function of pressure, the interpolated ($P^{0.5}{}_{H2}$ vs. n(H/Pd)) data were fitted with Equation (4-3) for several 0-n(H/Pd) intervals with n(H/Pd) as high as 0.1. Each 0-n(H/Pd) interval within which the interpolated data ($P^{0.5}{}_{H2}$ vs. n(H/Pd)) were fitted with Equation (4-3) corresponded to a 0-max. pressure interval. For instance, as seen in Figure 4-1, the 0-0.1n(H/Pd) interval corresponded to the 0-8.6 bar (=2.93 $bar^{0.5}$) pressure interval at 250ºC and 0-16.8 bar (=4.8 $bar^{0.5}$) pressure interval at 310ºC. Figure 4-2 shows the n-exponent values calculated for the 250, 290 and 310ºC isotherms as a function of the 0-max. pressure interval. The n-exponent increased as higher values of max. pressure were considered. That is, depending on the pressure range at which the H_2 flux is measured, J_{H2} is proportional to ($P^{0.5}{}_1$- $P^{0.5}{}_2$) at low pressures, for e.g. 1-2 bar, or J_{H2} is proportional to ($P^{0.6}{}_1$- $P^{0.6}{}_2$) in the 1-3.5 bar at 250ºC.

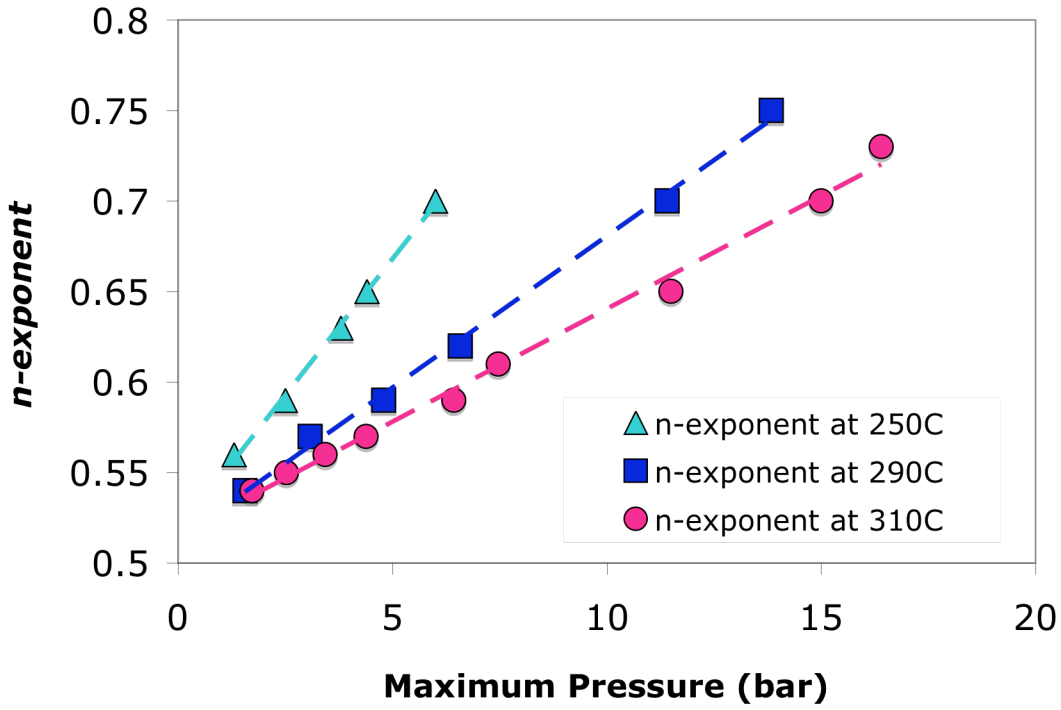

Figure 4-2 n-exponent as a function of maximum pressure for the 250, 290 and 310°C isotherms

The changes in the n-exponent due to the H_2 pressure range at which the H_2 flux is measured are denoted "pressure effects".

4.2.2 The permeation mechanism of H_2 through Pd foils

This section aimed at the establishment of the equation governing H_2 flux through Pd foils. H_2 permeation through Pd involves seven steps depicted in Figure 4-3: (1) H_2 diffusion from the bulk gas to the vicinity of the Pd surface, (2) dissociative adsorption onto the surface, (3) migration of atomic H on the surface into the bulk metal, (4) diffusion through the Pd lattice, (5) transition from the bulk metal to the surface on the permeate side, (6) associative desorption leading to H_2 molecules and (7) diffusion from the surface into the bulk gas. In the absence of external mass transfer, steps (1) and (7) can be neglected. In the case where steps (2)-(3) and (5)-(6) are at thermodynamic equilibrium, which is the case at temperatures higher than 150ºC, and for thick Pd foils (>1 μm), the H diffusion through the Pd lattice, step (4), is the rate-limiting step.

The H_2 flux is then given by Fick's first law, Equation (4-4).

$$J_{H_2} = \frac{D_H}{L_{Pd}}(n(H/Pd)_1 - n(H/Pd)_2) \qquad (4\text{-}4)$$

where J_{H2} is the H_2 flux in $m^3 \cdot m^{-2}\ h^{-1}$, D_H the H diffusivity through Pd in $m^2 \cdot h^{-1}$, L_{Pd} the thickness of the Pd layer in *m* and $n(H/Pd)_1$ and $n(H/Pd)_2$ the H concentrations at the high pressure side and at the low pressure side.

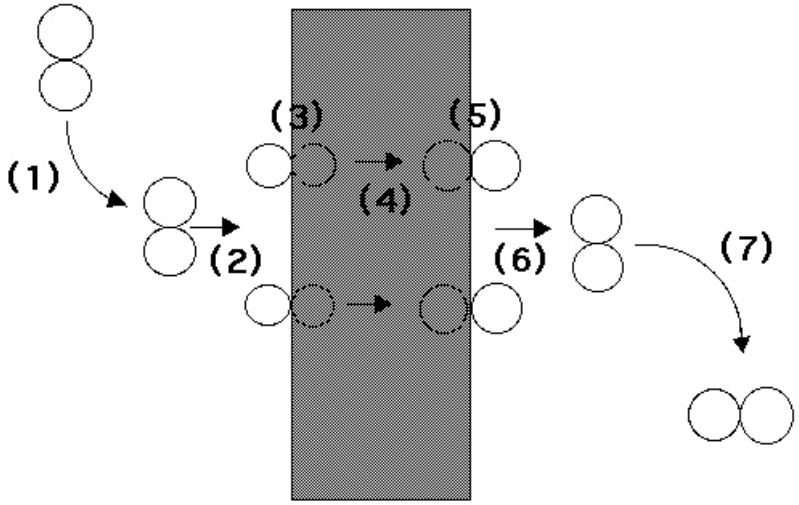

Figure 4-3 H_2 permeation through a freestanding Pd film

Substituting $n(H/Pd)_1$ and $n(H/Pd)_2$ in Equation (4-4) with the expression given in Equation (4-3) leads, after re-ordering, to Equation (4-5).

$$J_{H_2} = \frac{D_H(T) \cdot S_H(T)}{L_{Pd}} (P_1^{n-\exponent} - P_2^{n-\exponent}) \quad (4\text{-}5)$$

In Equation (4-5), S_H(T)=1/K'(T) is the H_2 solubility in the Pd lattice in $\cdot Pa^{-n\text{-}exponent}$. The product $D_H \cdot S_H$ is called H_2 permeability ($m^3\ m\ m^{-2} \cdot h^{-1} \cdot bar^{-n\text{-}exponent}$) and is the magnitude used to compare the H_2 permeation properties of different membranes. The H_2 permeability is temperature dependent via the H_2 diffusion coefficient, following the Arrhenius Equation (4-6), and via the solubility S_H, Equation (4-7)

$$D_H(T) = D_0 \cdot Exp(-\frac{E_{diff}}{R \cdot T}) \quad (4\text{-}6)$$

$$S_H(T) = S_0 \cdot Exp(\frac{\Delta_r H}{R \cdot T}) \quad (4\text{-}7)$$

In Equation (4-6) E_{diff} is the activation energy for H diffusion in $J \cdot mol^{-1}$, R the universal gas constant in $J \cdot mol^{-1} \cdot K^{-1}$ and T the absolute temperature in K. In Equation (4-7), $\Delta_r H$ is the enthalpy of absorption of H_2 in Pd in $J \cdot mol^{-1}$ *H.*

Combining Equations (4-5), (4-6) and (4-7), results in Equation (4-8)

$$J_{H_2} = \frac{Q_0}{L} e^{-\frac{E_p}{RT}} \cdot (P_1^{n-\exponent} - P_2^{n-\exponent}) \quad (4\text{-}8)$$

with

$$Q_0 = D_0 \cdot S_0$$
$$E_p = E_{diff} + \Delta_r H$$

where, E_p is the activation energy of H_2 permeation through Pd in $J \cdot mol^{-1}$. The H_2 flux is further written in terms of H_2 permeability, Q(T) as shown in Equation (4-9)

$$J_{H_2} = \frac{Q(T)}{L_{Pd}} (P_1^{n-\exponent} - P_2^{n-\exponent}) \quad (4\text{-}9)$$

The H_2 permeance is defined as $Q(T)/L_{Pd}$ and is the most important characteristic determined in a Pd foil or a composite Pd membranes. The H_2 permeance is determined as described in Section 3.2.3. Depending on the pressure range used for the determination of the H_2 permeance, "pressure effects" have a large or small contribution to the n-exponent (see Figure 4-2).

4.2.3 The H_2 permeability of clean Pd

The H_2 permeability of the α phase of Pd, given by Equation (4-10), was measured by several researchers on thick Pd foils. Table 4-1 lists the values of Q_0 and E_p reported by Balovnev (1974), Davis (1954), Koffler et al. (1969), Toda (1958), Morreale et al. (2003) and Howard et al. (2004). This section aimed at the establishment of an average value for the H_2 permeability of Pd considering as basis the raw data provided by the above-mentioned authors.

$$Q(T) = Q_0 \cdot e^{\frac{-Ep}{RT}} \tag{4-10}$$

Table 4-1 H_2 permeability for Pd measured in Pd foils in previous works

Q_0 $m \cdot m^3/(m^2\text{-}h\text{-}bar^{0.5})$	Ep kJ/mol	Temp. range ^0C	Press. range bar	Reference
9.821E-03	18.56	200-700	$2.6 \cdot 10^{-5}$-1	(Davis, 1954)
4.396E-03	13.46	170-290	0.047-0.83	(Toda, 1958)
5.612E-03	15.65	27 to 436	$4 \cdot 10^{-7}$-$6.7 \cdot 10^{-5}$	(Koffler et al., 1969)
6.547E-03	15.47	100 to 620	$3 \cdot 10^{-10}$-$6.7 \cdot 10^{-7}$	(Balovnev, 1974)
4.896E-03	13.81	350-900	1-27.6	(Morreale et al., 2003)
2.831E-03	12.97	350-900	1-27	(Howard et al., 2004)

For the determination of the H_2 permeability of Pd, all researchers listed in Table 4-1 considered the n-exponent factor equal to 0.5. In fact, Balovnev (1974), Davis (1954), Koffler et al. (1969) and Toda (1958) experimentally showed that at very low pressures

(see Table 4-1) the H_2 flux was given by Sieverts' law. The average value and the standard deviation for the H_2 permeability of Pd was calculated using the data in Table 4-1 as follows: (1) The Pd H_2 permeability was calculated at 200, 300, 350, 400, 450, 500 and 550ºC using Equation (4-10) and replacing Q_0 and E_p with the numerical values listed in Table 4-1 (six permeabilities values were calculated at each temperature). (2) At each temperature, the average of the six Pd H_2 permeabilities was calculated as well as the standard deviation. The natural logarithm of the averaged Pd H_2 permeability was then plotted as a function of 1/T in order to determine the Q_o and E_p of the average Pd H_2 permeability.

Figure 4-4 shows the calculated Pd H_2 permeability, using the raw data from works listed in Table 4-1, as well as the computed average Pd H_2 permeability, plotted in a logarithmic scale as a function of 1/T. The Pd H_2 permeability reported by authors in Table 4-1, equaled the calculated average Pd H_2 permeability within an error of 30%. Figure 4-5 shows the natural logarithm of the average Pd H_2 permeability, as well as the natural logarithm of the calculated Pd H_2 permeability, plotted as a function of 1/T.

The linear regression performed on the ln(average H_2 permeability) vs. 1/T data led to the expression of the average Pd H_2 permeability, Equation (4-11), that will be considered for the remaining of the thesis to be the Pd H_2 permeability of a Pd foil.

$$Q(T) = Q_0 \cdot e^{\frac{-Ep}{R \cdot T}} = 0.00533 \cdot e^{\frac{-14900}{R \cdot T}} \pm 0.3 \cdot 0.00533 \cdot e^{\frac{-14900}{R \cdot T}} \qquad (4\text{-}11)$$

Hence, the average Pd H_2 permeability pre-exponential factor, Q_0, was determined to be equal to 0.0053 $m^3 \cdot m/(m^2\ h\ bar^{0.5})$ and the activation energy for the average Pd H_2 permeability, E_p, was determined to be equal to 14.9 $kJmol^{-1}$.

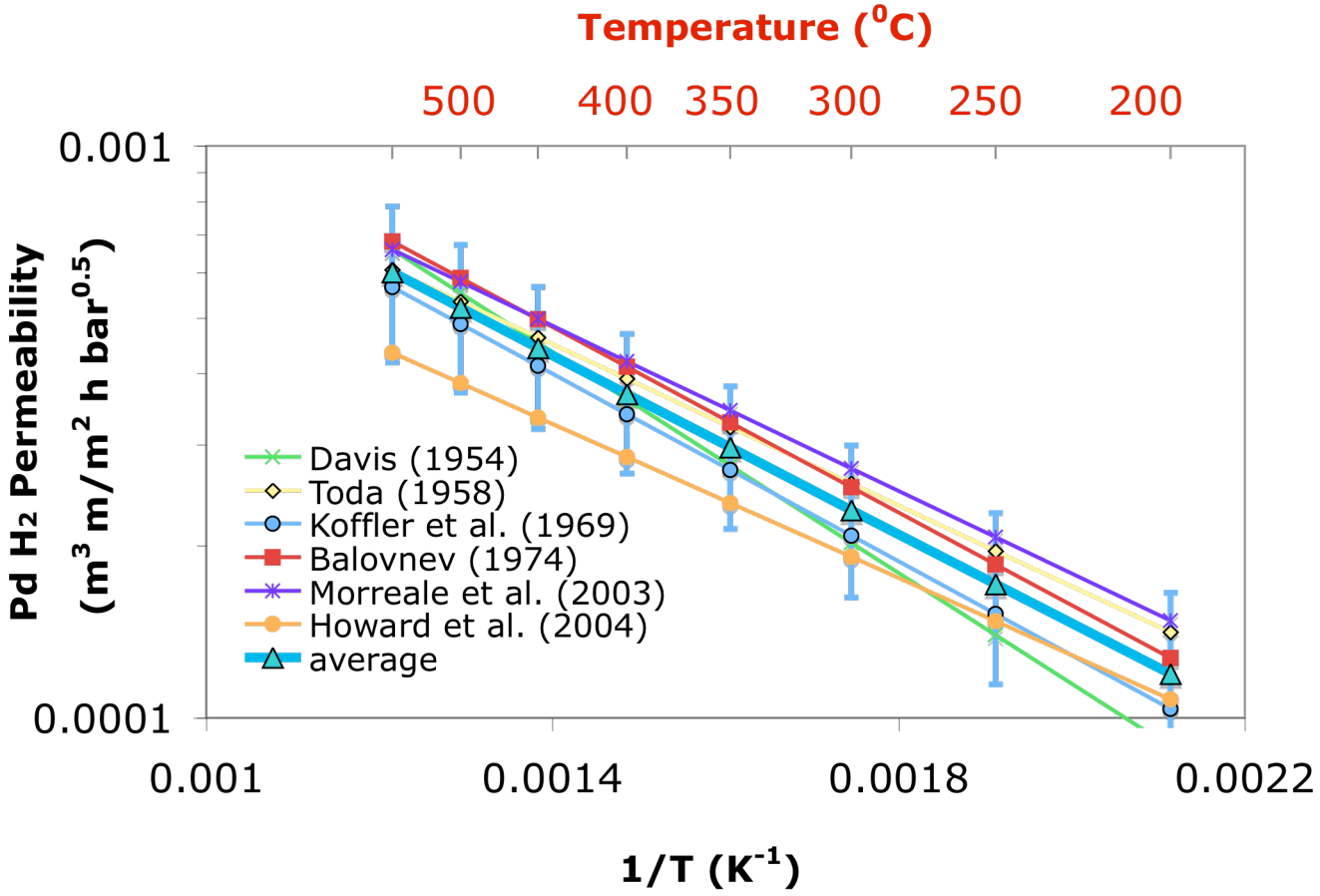

Figure 4-4 Pd H_2 permeability vs. 1/T for all references in Table 4-1

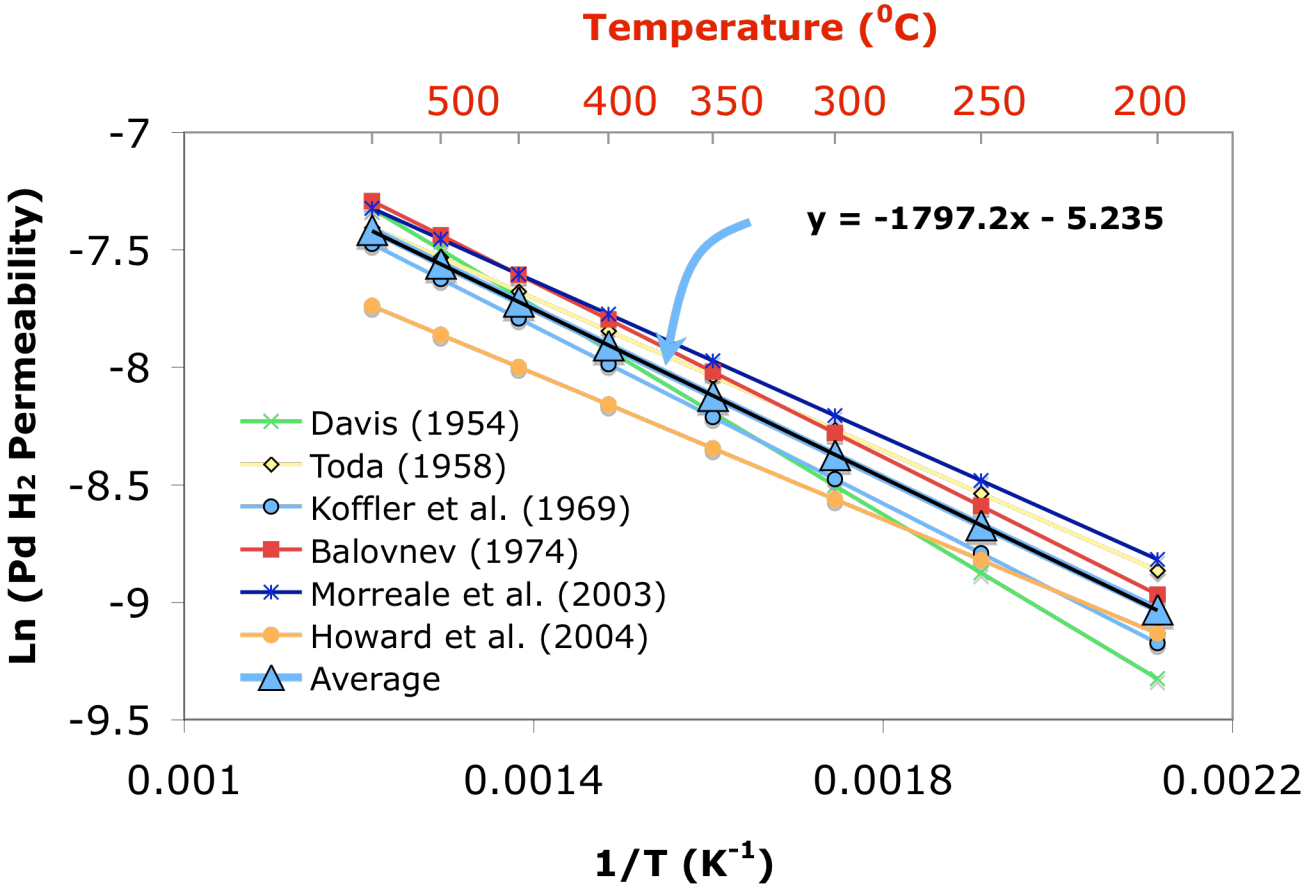

Figure 4-5 Ln(H_2 permeability) vs. 1/T for all references in Table 4-1

5 H_2 permeation through composite Pd membranes

5.1 Introduction

It has been largely accepted that H_2 flux through Pd films (foils and supported membranes) is governed by Equation (4-8).

$$J_{H_2} = \frac{Q_0 \cdot e^{-\frac{E_p}{R \cdot T}}}{L_{Pd}} \cdot (P_1^{n-\exponent} - P_2^{n-\exponent}) \qquad (4\text{-}8)$$

As already described in Chapter 4, H_2 permeation mechanism through a freestanding Pd film is a complex process involving several steps. The presence of a porous substrate on the low pressure side of this Pd film adds a degree of complexity, since H_2 also needs to flow through the porous media. Factors leading to deviations from Sieverts' law were already listed and are: the thickness of the Pd film when lower than 1 μm (Ward and Dao, 1999), surface poisoning, the presence of leaks, the presence of mass transfer resistance within the porous support and high H_2 pressures ("pressure effects"). All these factors alter the parameters in Equation (4-8) that can be determined from the measurement of H_2 flux as a function of pressure and temperature. These parameters are: the H_2 permeance F, the H_2 pressure exponent n-exponent and the activation energy for H_2 permeation E_P.

Surface poisoning, which is the adsorption of contaminants such as C, CO, CO_2 or hydrocarbons on the Pd surface, leads to a decrease in the adsorption rate of H_2. If the poisoning is too severe, reactions at the surface become the rate-limiting step for the H_2

permeation. Air oxidation at 300-450ºC was used for the removal of adsorbed CO, CO_2, methylcyclohexane (MCH), sulfur and chlorine in Pd-Ag membranes (Ali et al., 1994; Keuler and Lorenzen, 2002; Tosti et al., 2002). In some cases, an increase in H_2 permeance was observed (Ali et al., 1994) and was attributed to surface morphology changes. Auger spectroscopy of Pd thin foils was performed before and after air oxidation at 300ºC for 5 min (Yamakawa et al., 2003) and showed that carbon impurities (60at% on the surface) were removed as CO_2. Another important effect of air oxidation is the roughening of the Pd surface by the formation of a nano-structured oxide (Aggarwal et al., 2000; Han et al., 2004; Roa et al., 2003). An increase in surface area up to 50% was measured by Han et al. (2004) in Pd single crystals after exposure in oxygen at 600K, 1-150 torr for 10 min. Therefore, the overall effect of air oxidation resulted in a cleaner and rougher surface, which led to a highly activated Pd surface after reduction in H_2 atmosphere. The catalytic surface of Pd-6wt% Ru was modified by boiling in CCl_4, rinsing with HCl and annealing in H_2 at 700-800ºC, the H_2 permeance of the tube was enhanced by a factor of 2 and was attributed to the formation of an active porous layer due to the dissolution of the alloy components (Roshan et al., 1983). The H_2 permeability of Pd at low temperatures was also enhanced by the deposition of a thin layer (200 Å) of Pd black from glow discharges (Radzhabov et al., 1980). In both works (Radzhabov et al., 1980; Roshan et al., 1983) the increase in H_2 permeability was attributed to the increase of H dissolved in the inlet side of the membrane.

The H_2 flux through defects (cracks and/or pinholes in the Pd film), which is denoted as leaks, occurs via a mixed Knudsen-viscous mechanism (slip-flow) (Mardilovich et al., 1998). Therefore, the H_2 flux through defects can be expressed by the sum of a term pro-

portional to the pressure difference (Knudsen flow) and a term proportional to the square of the pressure (viscous flow). Hence, in a composite Pd membranes having large leaks the pressure exponent n-exponent will be higher than 0.5. Moreover, Knudsen-viscous mechanism is characterized by the activation energy of gas diffusion, which is lower compared to the activation energy of solution diffusion. Therefore, if large leaks are present, the activation energy for H_2 permeation will be lower than 12-20 kJ/mol (see Table 4-1).

Mass transfer within the porous support adds another resistance to the overall H_2 permeation mechanism. If L_{Pd} is thin enough and the porous support does not have a high inert gas permeance, which is the case in supports having a low porosity, the pressure drop within the porous support is high and the H_2 diffusion within the porous media becomes the rate-limiting step for the H_2 permeation. If H_2 diffusion through the porous media is the rate-limiting step, the pressure exponent n-exponent is higher than 0.5 and the activation energy for H_2 permeation decreases.

The primary objective of the models and experiments described in this chapter was to investigate the factors affecting the mechanism of H_2 permeance through composite Pd membranes. The effects of leaks and mass transfer within the porous support were modeled to determine the conditions under which the H_2 permeation mechanism would be strongly affected by leaks or mass transfer. The relation between the Pd surface activity and the n-exponent was also studied.

5.2 Theory

5.2.1 The model of mass transfer within the porous support

The model described in this section has the aim of estimating to what extent and in what manner mass transfer resistance within the support influences on the H_2 permeation, the H_2 pressure n-exponent and the activation energy for H_2 permeation E_p. The thickness of the thin Pd film was always negligible compared to the outside diameter (OD) of the support, therefore, the mass transfer equations were written in a planar geometry. A sketch of a composite Pd/substrate structure is given in Figure 5-1.

The H_2 flux through the dense Pd layer, J_1, is given by Sieverts' law, Equation (5-1).

$$J_1 = \frac{Q(T)}{L_{Pd}} \cdot (P_1^{0.5} - P_2^{0.5}) \tag{5-1}$$

with $Q(T)$ the H_2 permeability in $m^3/(m^2\ h\ bar^{0.5})$ at the temperature T, L_{Pd} the membrane thickness and P_1 and P_2 the high and low H_2 pressure. The average Pd H_2 permeability $Q(T)$ was estimated in Section 4.2.3 and is given by Equation (4-11).

$$Q(T) = Q_0 \cdot e^{\frac{-Ep}{R \cdot T}} = 0.00533 \cdot e^{\frac{-14900}{R \cdot T}} \tag{4-11}$$

The H_2 flux through the porous support, J_2, was given by the dusty-gas model as shown in Equation (5-2). This approach was also undertaken to study the mass transport in asymmetric alumina membranes (Thomas et al., 2001).

$$\begin{aligned} J_2 &= [\alpha_{H_2}(T) + \beta_{H_2}(T) \cdot (\frac{P_2 + P_3}{2})] \cdot (P_2 - P_3) \\ &= [\frac{2}{6}\sqrt{\frac{8}{\pi}} \frac{\varepsilon \mu_k d}{L_{subs}\sqrt{RTM_{H_2}}} + \frac{1}{32} \frac{\varepsilon \mu_v d^2}{L_{subs}\eta_{H_2} RT} \cdot (\frac{P_2 + P_3}{2})] \cdot (P_2 - P_3) \end{aligned} \tag{5-2}$$

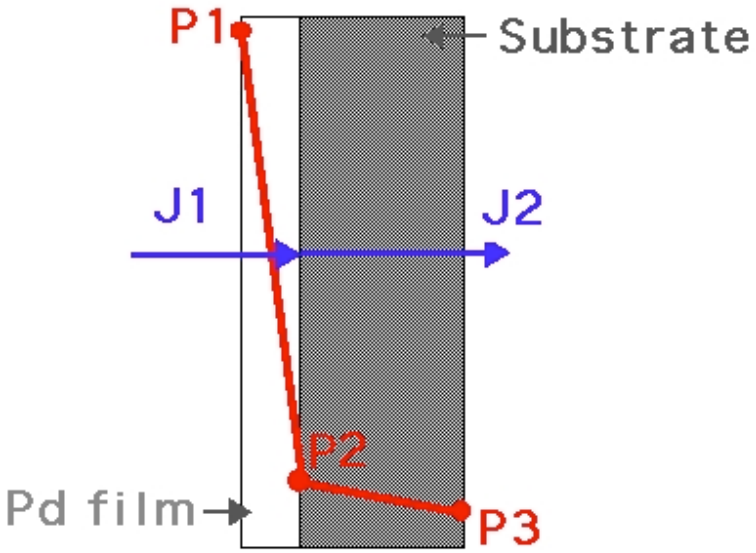

Figure 5-1 Scheme of a composite Pd-porous substrate structure.

The $\alpha_{H2}(T)$ and $\beta_{H2}(T)$ parameters were determined from He permeation measurements at room temperature (T=293K). The He flux of the bare support, without the Pd coating, was measured at 5-10 different pressures P_1 after the grading step or after the oxidation step. The permeate pressure, P_2, was kept at atmospheric conditions. The raw data (J_{He}, P_1) were then plotted in the ($J_{He}/(P_1-P_{atm})$, $(P_1+P_{atm})/2$) form and fitted with Equation (5-2) to finally obtain $\alpha_{He}(293)$ and $\beta_{He}(293)$. Figure 5-2 shows the experimental data ($J_{He}/(\Delta P)$, P_{ave}) collected after the grading of C01-F11a/b membrane' s support as an example. It was also possible to measure $\alpha_{H2}(293)$ and $\beta_{H2}(293)$, and even $\alpha_{H2}(T)$ and $\beta_{H2}(T)$ at different temperatures. However, the measurement of $\alpha_{H2}(T)$ and $\beta_{H2}(T)$ required to place the bare support in a reactor, which implied the same safety procedures as when characterizing membranes. Therefore, for simplicity reasons $\alpha_{H2}(T)$ and $\beta_{H2}(T)$ were determined using $\alpha_{He}(293)$ and $\beta_{He}(293)$.

$\alpha_{H2}(T)$ and $\beta_{H2}(T)$ were readily calculated from $\alpha_{He}(293)$ and $\beta_{He}(293)$ by substituting M_{He} and η_{He} in the expression of α_{He} and β_{He} parameters using Equation (5-3).

$$\begin{aligned} J_2 &= [\alpha_{H_2}(T) + \beta_{H_2}(T)\frac{P_2 + P_3}{2}]\cdot(P_2 - P_3) \\ &= [\alpha_{He}(293)\cdot\sqrt{\frac{293}{T}}\sqrt{\frac{M_{H_e}}{M_{H_2}}} + \beta_{He}(293)\cdot\frac{293}{T}\frac{\eta_{He}(293)}{\eta_{He}(T)}\frac{\eta_{He}(T)}{\eta_{H_2}(T)}(\frac{P_2 + P_3}{2})]\cdot(P_2 - P_3) \end{aligned} \quad (5\text{-}3)$$

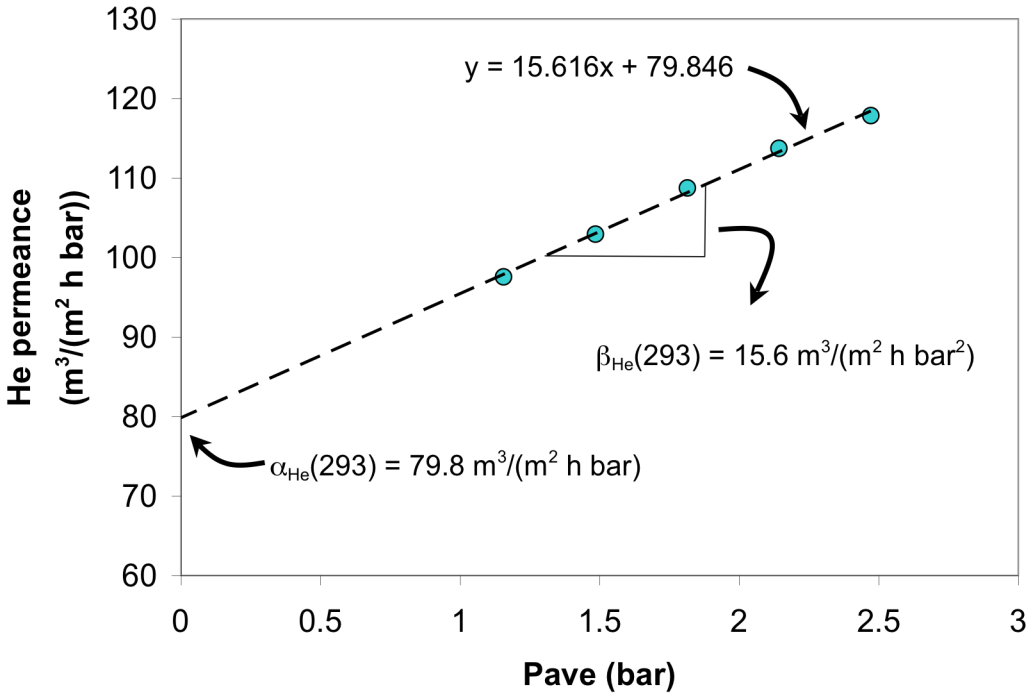

Figure 5-2 He permeance vs. P_{ave} for the graded support of C01-F11a/11b membranes

The ratio η_{He}/η_{H2} was taken to be equal to 2.29, which was the average ratio of the He viscosity over the H_2 viscosity in the 20-500ºC temperature range. At steady state J_1 equals to J_2 leading to Equation (5-4).

$$\frac{Q(T)}{L_{Pd}} \cdot (P_1^{0.5} - P_2^{0.5}) = [\alpha_{H_2}(T) + \beta_{H_2}(T) \cdot (\frac{P_2 + P_3}{2})] \cdot (P_2 - P_3) \qquad (5\text{-}4)$$

The calculations were performed as follows. (1) L_{Pd}, known from gravimetric measurements or SEM micrographs, and the temperature T were set, (2) a given H_2 pressure value ranging within the 0-5 bar was given to P_1, (3) P_3 was kept equal to 1 bar, (4) P_2, the only unknown in Equation (5-4), was solved numerically and, (5) the H_2 flux was then computed using either Equation (5-1) or Equation (5-2). For each temperature T, ten H_2 fluxes were computed at the following P_1 pressures: 1.2, 1.5, 2, 2.5, 3, 3.5, 4, 4.5, 5 and 5.5 bar. The computed data (J_{H2}, P_1, P_3) were then fitted with Equation (3-2) to determine $F_{0.5}$ and with Equation (3-3) to determine the F_n and the n-exponent.

$$J_{H_2} = F_{0.5} \cdot (P_1^{0.5} - P_3^{0.5}) \qquad (3\text{-}2)$$

$$J_{H_2} = F_n \cdot (P_1^{n-\exponent} - P_3^{n-\exponent}) \qquad (3\text{-}3)$$

Mass transfer limitations arise when the H_2 flux through the Pd layer is too large compared to the H_2 flow the support can convey without large pressure drops. That is, a parameter, ξ, that compares the resistance for the H_2 flux through the Pd layer and the resistance for the H_2 flux through the porous support, gives information on the presence of mass transfer effects in a composite Pd membrane. ξ was defined by the ratio of the resistance of H_2 flux through the Pd layer (ΔP=1 bar, $\Delta P^{0.5}$=0.4142 $bar^{0.5}$) over the resistance of the H_2 flux through the support (ΔP=1 bar, P_{ave}=1.5 bar) both estimated from H_2 fluxes at 250ºC and ΔP=1 bar (2:1). ξ_{250} is given by Equation (5-5).

$$\xi_{250} = \frac{R_{Pd}}{R_{\sup port}} = \frac{\left(\frac{1}{J_{H_2,Pd}}\right)_{\Delta P=1,250C}}{\left(\frac{1}{J_{H_2,\sup port}}\right)_{\Delta P=1,250C}} = \frac{[\alpha_{H_2}(T) + \beta_{H_2}(T)\frac{P_1+P_2}{2}]\cdot(P_1-P_2)}{\frac{Q(T)}{L_{Pd}}\cdot(P_1^{0.5}-P_2^{0.5})}$$

$$with,\ \ T = 523\cdot K,\ \ P_1 = 2\cdot bar,\ \ P_2 = 1bar \qquad (5\text{-}5)$$

$$\xi_{250} = \frac{[\alpha_{He}(293)\cdot\sqrt{\frac{293}{523}}\sqrt{\frac{M_{He}}{M_{H_2}}} + \beta_{He}(293)\cdot\frac{293}{523}\frac{\eta_{He}(293)}{\eta_{He}(523)}\frac{\eta_{He}(523)}{\eta_{H_2}(523)}(\frac{3}{2})]\cdot 1}{\frac{Q(523)}{L_{Pd}}\cdot(\sqrt{2}-1)}$$

5.2.2 The leak model

In a composite Pd membrane, H_2 diffuses through the lattice of palladium, along the Pd grain boundaries and also along the defects within the thin Pd layer. Figure 5-3, shows the diffusion of H through the Pd lattice according to a "solution diffusion" mechanism and the diffusion of molecular hydrogen (H_2) along defects in a Pd thin film.

The flow of H_2 through defects can lead to the overestimation of the H_2 that permeates through the "solution diffusion" mechanism. This section describes a model that provides the basis for the establishment of the minimum selectivity (H_2/He) a composite Pd membrane should have in order to consider the effects of leaks on the H_2 permeating according to the "solution diffusion" mechanism negligible. The minimum selectivity is determined is Section 5.4.2.

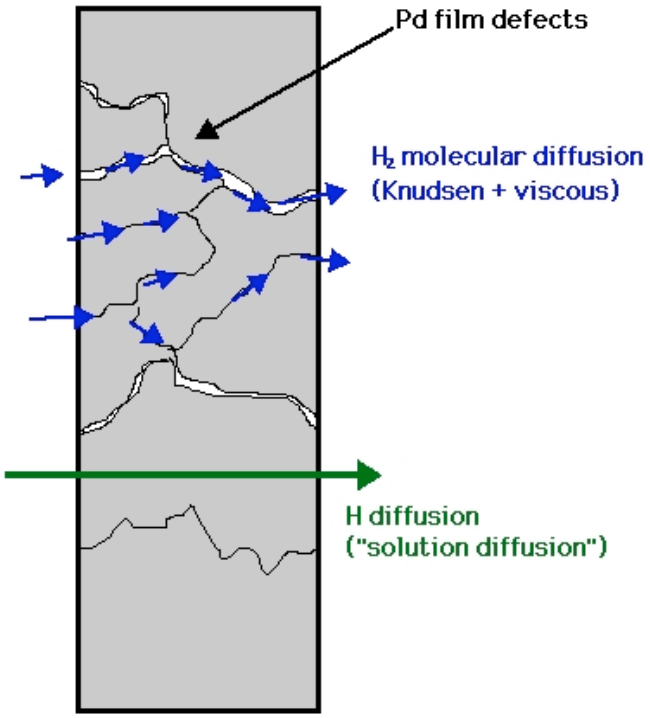

Figure 5-3 The diffusion of H through Pd lattice ("solution diffusion") and the diffusion of H_2 through defects

The total H_2 flux permeating through the Pd foil, shown in Figure 5-3, is equal to the sum of the H_2 permeating according to the "solution diffusion" mechanism and the H_2 permeating along the defects. The model is based on the following assumptions:

- The H_2 flux permeating according to the "solution diffusion" mechanism is independent on the selectivity value. The H_2 permeance of the freestanding Pd foil is set equal to 10 $m^3/(m^2\ h\ bar^{0.5})$. The H_2 flux permeating through the Pd lattice follows Sieverts' law.
- Molecular H_2 diffuses through the defects according to a mixed Knudsen-viscous mechanism. The amount of H_2 flowing through defects was estimated from the flow of He (the He leak) diffusing through the defects. The same approach was taken by Mardilovich et al. (1998) to describe inert gas flow through composite Pd membranes with defects.

The calculations were performed according to the following procedure:

(1) A selectivity value, which was assumed to be determined at a ΔP=1bar (2:1), was set.

(2) The He flux, J_{He}, at a ΔP=1bar (2:1) was calculated according to equation (5-6).

$$J_{He} = \frac{F_{0.5} \cdot \Delta P^{0.5}}{Selectivity} \qquad (5\text{-}6)$$

In Equation (5-6), $\Delta P^{0.5}$ stands for $P^{0.5}_{shell} - P^{0.5}_{tube}$. For the calculations, P_{shell} was set to 2 bar and P_{tube} was set to 1 bar. As already mentioned, the H_2 permeance of the freestanding Pd foil, $F_{0.5}$, was set equal to 10 $m^3/(m^2\ h\ bar^{0.5})$.

(3) The He flux, J_{He}, was equal to the sum of a Knudsen, α, and a viscous, $\beta \cdot P_{ave}$, contribution according to Equation (5-7).

$$J_{He} = [\alpha \cdot + \beta \cdot P_{ave}](\Delta P) \quad (5\text{-}7)$$

An r value was set to calculate α and β. Indeed, in order to calculate α and β the contribution of the Knudsen flow to the overall leak had to be set. Therefore, r values ranging from 0 (leak dominated by viscous flow) to 1 (leak dominated by Knudsen flow) were assumed for the calculations. α, β and r are given by Equation (5-8).

$$r = \frac{\alpha}{\alpha + \beta \cdot P_{ave}}$$
$$\alpha = r \cdot \frac{J_{He}}{\Delta P} \quad (5\text{-}8)$$
$$\beta = \frac{J_{He}}{\Delta P} \cdot \frac{(1-r)}{P_{ave}}$$

where ΔP and P_{ave} are the pressure difference and average pressure at which the He leak was assumed (ΔP=1 bar and P_{ave}=1.5 were used in the calculations).

(4) the total H_2 flux (the sum of the H_2 flowing through defects and the H_2 flowing through the Pd lattice) was estimated at several P_{shell} values in the 0.2-4.5 bar pressure range according to Equation (5-9). P_{tube} was always set to 1 bar.

$$J_{H2} = F_{0.5} \cdot (\Delta P^{0.5}) + [\alpha \cdot \sqrt{\frac{M_{He}}{M_{H2}}} \cdot + \beta \cdot \frac{\eta_{He}}{\eta_{H2}} \cdot P_{ave}](\Delta P) \quad (5\text{-}9)$$

In Equations (5-9), the H_2 flux is the sum of a solution diffusion term, a Knudsen term and viscous term. All pressures in Equation (5-9) are H_2 partial pressures. For the sake of simplicity, the coefficient (η_{He}/η_{H2}) was assumed to be 2.29, which was the average ratio of the He viscosity over the H_2 viscosity in the 250-500ºC temperature range.

Figure 5-4 shows as example the calculated J_{H2} for r = 0 and a selectivity value of 40. At high pressures, the calculated J_{H2} (r=0, selectivity=40) deviates significantly from the J_{H2} this hypothetical Pd film would show at infinite selectivity i.e. for the calculated J_{H2} with selectivity=∞. The same type of data was computed for r=0, 0.2, 0.4, 0.6, 0.8 and 1 and selectivity=10, 20, 30, 40, 50, 100, 200, 300 and 400.

All computed (H_2 flux, P_{shell}) data were then fitted with Equation (3-2) to determine H_2 permeance assuming Sieverts' law ($F_{0.5}$), and also with Equation (3-3) to determine H_2 permeance (F_n) and the n-exponent as described in Section 3.2.3.

5.3 Experimental

Membranes C01-F03/4/5/7 were prepared on non-graded supports following the preparation procedure described in the experimental Chapter 3. Membranes C01-F08, C01-F011, C01-F011b, Ma-32, Ma-32b, Ma-34b, Ma-41 and Ma-42 were prepared on "graded" supports.

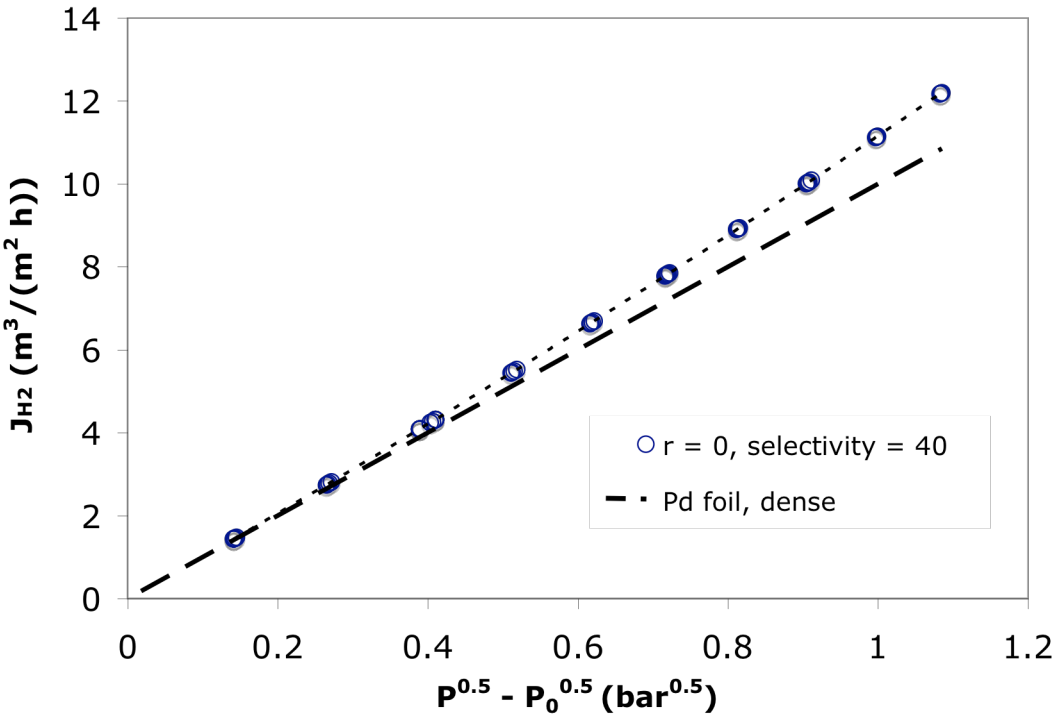

Figure 5-4 Calculated J_{H2} as function of ($P^{0.5}$-$P^{0.5}{}_0$) with r=0 and selectivity =40 (open circles) and selectivity =∞ (dashed line).

The graded supports were synthesized according to the experimental protocol described in Section 3.1.2. For membranes Ma-32, Ma-32b, Ma-34b and Ma-42 only the mass transfer within their porous supports was studied in order to provide sufficient proof for the mass transfer model presented in Section 5.2.1. The particular structure and H_2 permeation properties of membranes Ma-32, Ma-32b, Ma-34b and Ma-42 will be discussed in great detail in Chapter 6.

5.4 Results and discussion

5.4.1 The relevance of the n-exponent in this work

This section aims at understanding the relevance of the n-exponent. As an example, the experimental results from composite Pd membrane C01-F03 are shown.

Figure 5-5 shows the H_2 flux at 300ºC for membrane C01-F03 as a function of the Sieverts' driving force ($P^{0.5}_1$- $P^{0.5}_2$). The H_2 permeance at 300ºC, assuming that the Sieverts' law was followed, was 6.83 $m^3/(m^2\ h\ bar^{0.5})$. Residuals ($H_{2\ exp\ flux} - H_{2\ calc\ flux}$) are also plotted as a function of the Sieverts' driving force in Figure 5-5 (squares) and showed a distinctive polynomial trend. The same trend was found at all temperatures at which all membranes were tested, indicating that the Sieverts' law was not followed and that the pressure exponent was different from 0.5. The H_2 permeance had therefore to be determined by adjusting the n-exponent (Equation (3-3)). Adjusting the n-exponent resulted in a H_2 permeance equal to 5.0 $m^3/(m^2\ h\ bar^{0.63})$ and an n-exponent equal to 0.63. The residuals (crosses in Figure 5-5) lie very close to the value of zero indicating a better fit.

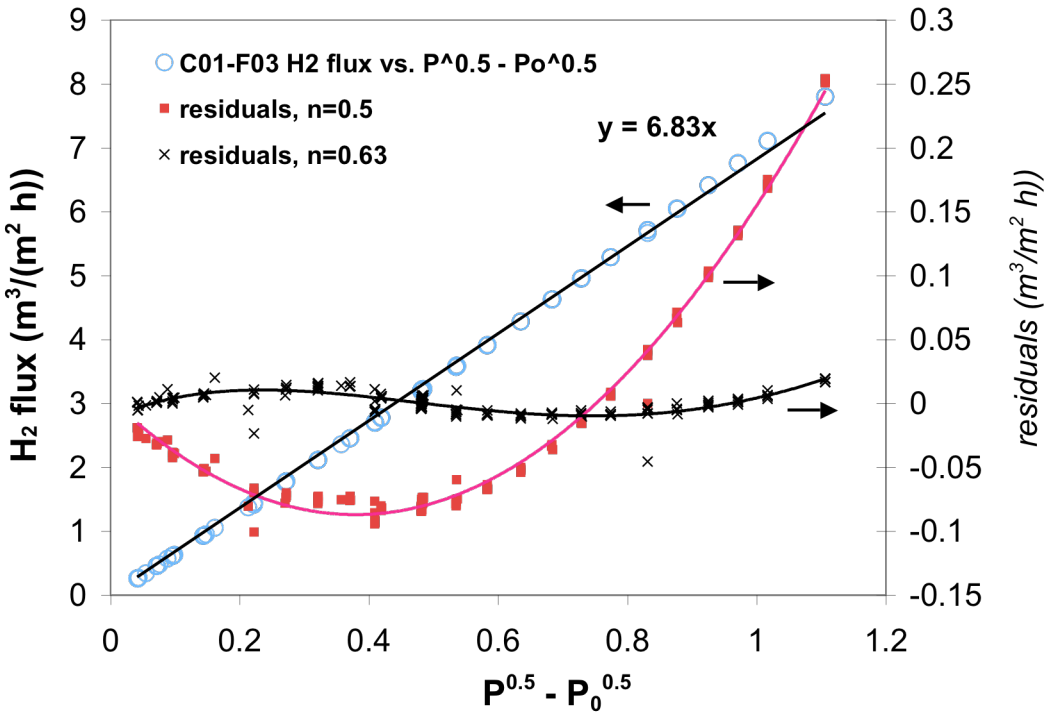

Figure 5-5 H_2 flux and residuals as a function of $P^{0.5}$-$P^{0.5}{}_0$ at 300ºC for membrane C01-F03.

The natural logarithm of the H_2 permeance of membrane C01-F03, calculated by both methods (linear fit with n=0.5 and non-linear regression to determine *n-exponent* and F_n), is plotted in Figure 5-6 as a function of 1/T. The slight decrease of the permeance above 325ºC was due to intermetallic diffusion. Figure 5-6 shows two temperature regions: the 250-400ºC temperature interval, which was characterized by a fast decrease in the n-exponent and a second temperature window 400-500ºC, which was characterized by a rather constant n-exponent.

The n-exponent of membrane C01-F03 decreased as the temperature was increased. At 250ºC the n-exponent was equal to 0.66 and decreased to 0.55 at 400ºC. The n-exponents within the 250-400ºC temperature range were higher than the n-exponents predicted by calculations performed on the experimental isotherms (see Figure 4-1 and Figure 4-2). The high n-exponents measured for C01-F03 were due to the adsorption of impurities on the Pd surface, thereby decreasing the rate of H_2 absorption/desorption reactions. The n-exponents of C01-F03 decreased as temperature was increased following the trend predicted by the calculations on the Pd-H phase diagram (see Figure 4-2). At temperatures higher than 400ºC the pressure exponent of C01-F03 was very close to 0.5 as shown in Figure 5-6. It is interesting to note that the pressure effects (the increase in the n-exponent due to the determination of the H_2 permeance in the 0-4.5 bar pressure range) vanished at a temperature higher than 350ºC, which was in agreement with the predictions of Ward and Dao (1999).

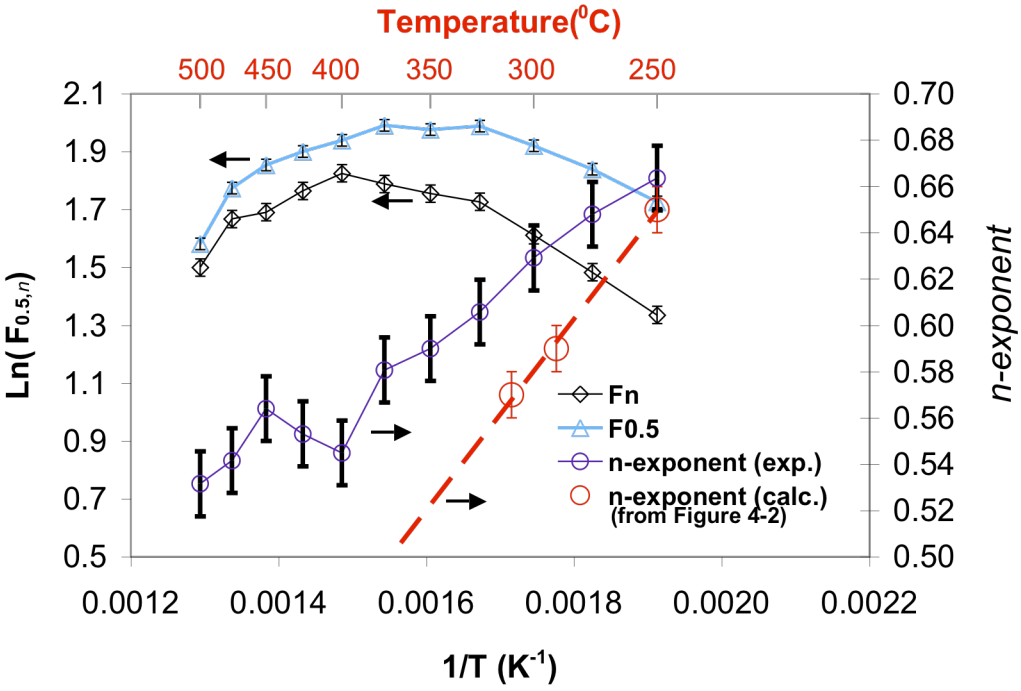

Figure 5-6 Ln(F_n), Ln($F_{0.5}$) and n-exponent for membrane C01-F03 as a function of 1/T.

The decrease of the n-exponent seen for membrane C01-F03 in the 250-400ºC temperature range has also been reported by several authors. Decreasing n-exponents from 0.62 at 450ºC to 0.55 at 600ºC were reported by Collins and Way (1993) on composite Pd-Al_2O_3 membranes. The decrease in n-exponent was attributed to the removal of surface contaminants present on the fresh surface of the membrane. However, n-exponents reported by Collins and Way (1993), were higher than n-exponents seen in membrane C01-F03 at 450ºC. The difference in n-exponents was due to the wider pressure range considered by them (up to 27 bar).

Deviations from the Sieverts' law at temperatures lower than 400ºC (see Figure 5-6) were mainly attributed to the non-linear H_2 absorption isotherms (high H_2 pressure effects) and secondly to the poor catalytic properties of the Pd surface due to the presence of contaminants adsorbed on the surface. The contaminant adsorbed on the surface of fresh composite Pd membranes come form the plating bath, which contains EDTA and ammonia. Theoretically the n-exponent should have been equal to 0.5 (Sieverts' law) at 500ºC however, imperfections formed at high temperatures leading to Knudsen and viscous flow. Indeed, the selectivity (H_2/He) of membrane C01-F03 was just above 100 at the end of the characterization. Indeed, Section 5.4.2 shows that the n-exponent is higher than 0.5 in membranes having selectivities lower than 300. Membranes C01-F03/4/5, which were proven to have no mass transfer limitations (see Section 5.4.3.2), had n-exponent values around 0.6 at 250ºC and around 0.53 at 500ºC. Hence the n-exponent value decreased as temperature was increased for all composite Pd membranes characterized in this study.

It is important to acknowledge the fact that the n-exponent value is slightly different form 0.5 and that the n-exponent is a decreasing function of the temperature. Although, in order to be able to compare the H_2 permeance of all membranes, and also, in order to be able to determine the activation energy for H_2 permeation in any temperature range, Sieverts' law is required to be assumed. The assumption of Sieverts' law is valid since the experimental n-exponents were very close to 0.5. Moreover, all composite Pd membranes prepared in this work had dense Pd layers thicker than 5 μm, were tested at temperatures higher than 250ºC and feed H_2 pressures higher than 1 bar. Therefore, the rate-limiting step for H_2 permeation was the H diffusion through Pd bulk according to calculations performed by Ward and Dao (1999). From this point in the thesis, the H_2 permeance of any composite Pd membrane will be determined assuming the H_2 flux is proportional to $(P^{0.5}-P^{0.5}{}_0)$ and $F_{0.5}$ will be determined fitting $(J_{H2}, (P^{0.5}-P^{0.5}{}_0))$ data with Equation (3-2). Also, the n-exponent, which was always calculated for verification purposes, was used as a tool to understand if any other effect such as leakages, mass transfer resistance within the support or surface activity, had a strong influence on the H_2 permeation mechanism. For all composite Pd membranes prepared in this work, H diffusion through the Pd bulk was the rate-limiting step for hydrogen permeation in the absence of mass transfer, leakages and clean surfaces.

5.4.2 The effects of leaks on H_2 flux

This section aimed at the establishment of the minimum selectivity a composite Pd membrane should have in order to consider the effects of leaks on the determination of the H_2 permeating according to the "solution diffusion" mechanism negligible. The results obtained from the He leak model in Section 5.2.2 are discussed.

Figure 5-7(a) shows the H_2 permeation F_n as a function of selectivity (H_2/He at ΔP=1bar, see Equation (5-6)) for r values ranging between 0 and 1 for the hypothetical Pd foil of Section 5.2.2. Figure 5-7(b) shows the n-exponents as a function of selectivity (H_2/He at ΔP=1bar) for the same r values. The presence of leaks led to the increase of the H_2 pressure exponent. The area between r=0 and r=1 curves can be denoted as the leak envelope and for any experimental point (n-exponent, selectivity) lying in such an envelope its n-exponent is essentially explained by the leak of the membrane. For example, from Figure 5-7(b) the n-exponent of a composite Pd membrane with a selectivity of 300 and r=0 is 0.52. An n-exponent of 0.52 is considered to be equal to 0.5, since n-exponents were determined with a precision of 0.02. Therefore, it can be concluded that when the selectivity of a membrane is above 300, leaks do not have any significant effect on either H_2 permeance or n-exponent. In other words, if n>0.50 and the selectivity is higher than 300 the reasons for n>0.5 are due to factors other than defects.

From the measurement of the He permeance in all membranes and at many temperatures, it was found that r was never lower than 0.6. If we now consider r equal to 0.6, the necessary selectivity to make the n-exponent increase by 0.02 units (0.02 was the precision achieved in the determination of the n-exponent) was around 150-200 as seen in Figure 5-7(b). Therefore, the effects of leaks in a composite Pd membrane with a selectivity of 200 or higher were considered as negligible on the n-exponent and the H_2 permeance $F_{0.5}$.

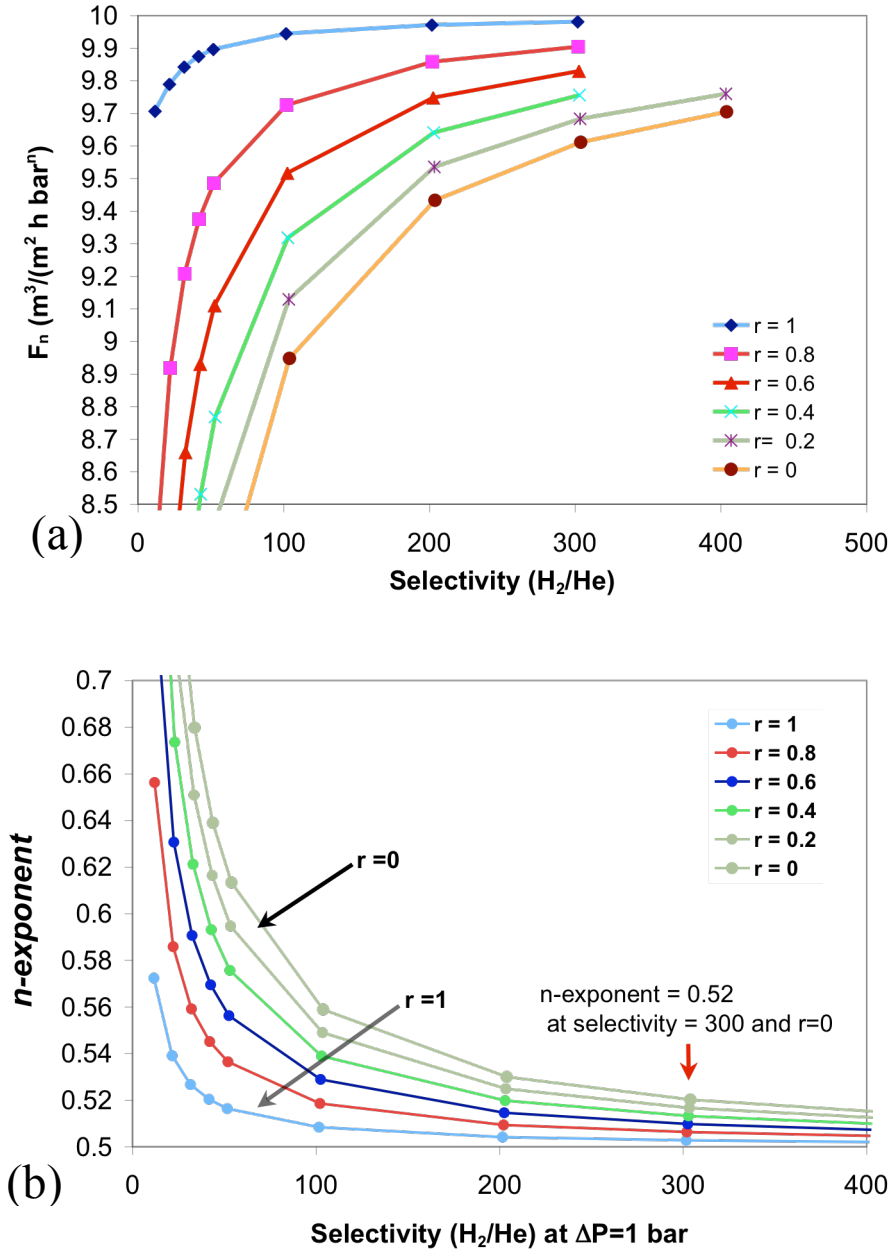

Figure 5-7 (a) F_n vs. selectivity (b) n-exponent vs. selectivity for different r ratios

Figure 5-8 shows the H_2 permeance of the Pd film in Section 5.2.2 one would measure ($J/(P_1^{0.5}-P_3^{0.5})$) assuming Sieverts' law is valid (n=0.5) for different values of r.

As expected the presence of leaks led to an overestimation of the real H_2 permeance (10 $m^3/(m^2\ h\ bar^{0.5})$). For a membrane having a selectivity of 200 and a leak with a Knudsen contribution equal to or higher than 0.6, the computed overestimation in H_2 permeance was only equal to 1.3% of the film's true H_2 permeance. The H_2 permeance was measured within a precision of 2%, which was higher than the computed increase in H_2 permeance due to the leak. Hence, as already stated, leaks did not have significant effects on the measurement of H_2 permeance and n-exponent when the selectivity was over 200 measured at ΔP=1 bar (2:1).

In order to understand the effect of membrane defects on the H_2 permeation and also to validate the n-exponent/selectivity model, two composite Pd membranes, C02-F01 and C02-F03, with large defects were studied. Their initial He leak at 250ºC just before the H_2 introduction was high and equaled $2.95\cdot10^{-3}$ $m^3/(m^2\ h\ bar)$ for C02-F01 and $1.06\cdot10^{-3}$ $m^3/(m^2\ h\ bar)$ for C02-F03. The He leak and selectivity were determined at each temperature after changing from H_2 to He. Two measurements of the He leak were performed at each temperature separated by 24 hr. The calculated n-exponents and selectivities as a function of temperature are plotted in Figure 5-9 for both membranes. As expected, the membrane having the larger defects (large He leak) showed higher n-exponents at any given temperature.

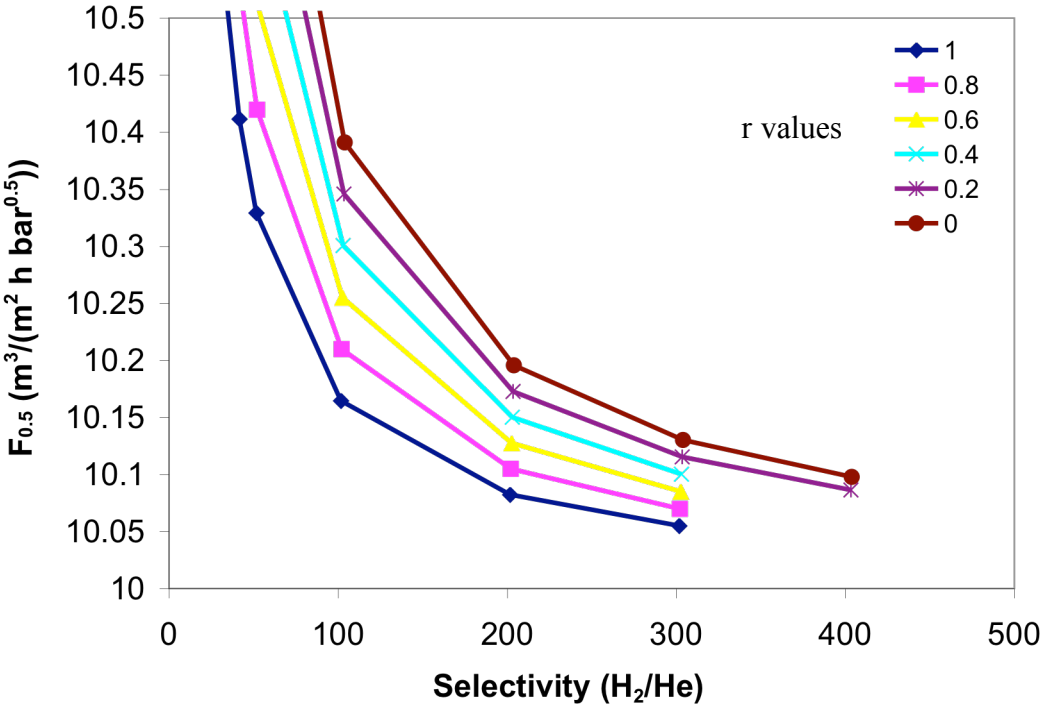

Figure 5-8 $F_{0.5}$ vs. selectivity for different values of r

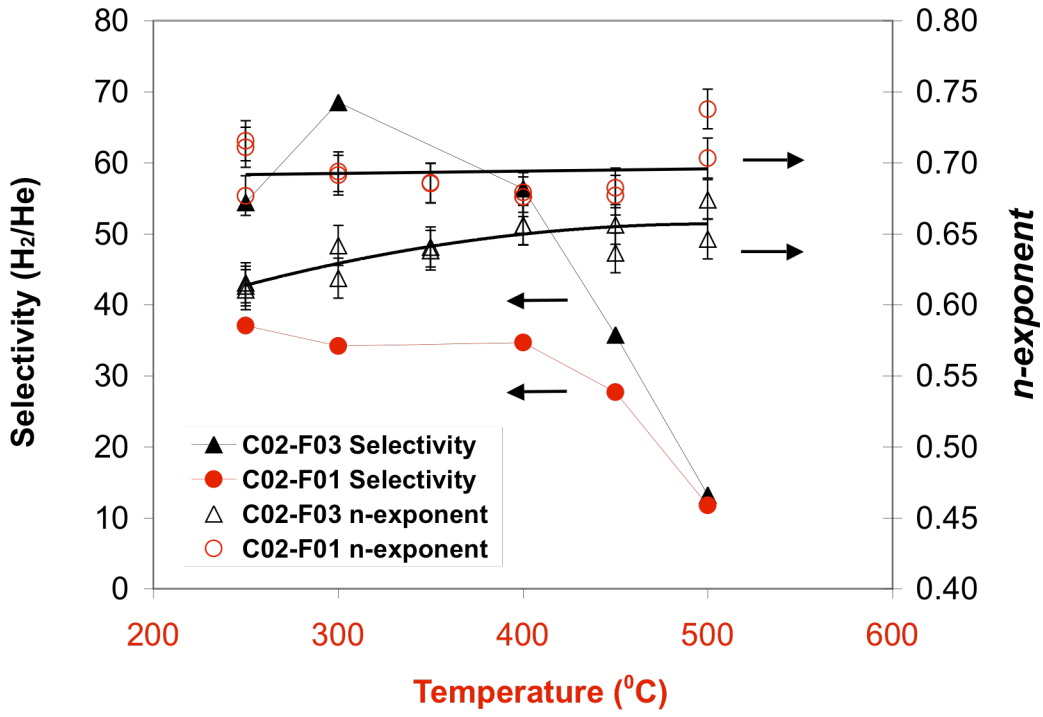

Figure 5-9 Selectivity and n-exponent vs. temperature for C02-F01 and C02-F03 membranes

The n-exponent of membrane C02-F03 increased rather slowly with increasing temperature from 0.61 at 250ºC to 0.66 at 450ºC. The n-exponent of membrane C02-F01 remained constant from 250ºC to 450ºC (0.68-0.70) and increased afterwards up to 0.74 at 500ºC. Interestingly, the n-exponent at 500ºC increased by 0.03 units between the first and second measurement for both membranes (24 hr interval) indicating the rapid growth of the He leak at 500ºC.

Figure 5-10 shows the n-exponent as a function of the selectivity for membranes C02-F01 and C02-F03. Each experimental point corresponds to the temperature shown next to the point. It can be seen that all experimental data points lie very close or within the leak envelope. When selectivities reached 10-20 the higher n-exponents were attributed to large defects in the Pd layer.

5.4.3 The effects of mass transfer resistance in the support on H_2 flux

5.4.3.1 Modeling the H_2 mass transfer within the porous metal support

It was rather difficult to determine from the characteristics of a given membrane (H_2 permeation, H_2 pressure exponent, activation energy for H_2 permeation) if the mass transfer resistance across the porous support accounted for a large portion of the total resistance for H_2 permeation. That difficulty in assessing the possible contribution of mass transfer resistance to the overall resistance was due to the small variations that the mass transfer resistance induced on the H_2 permeance, activation energy for H_2 permeation and n-exponent.

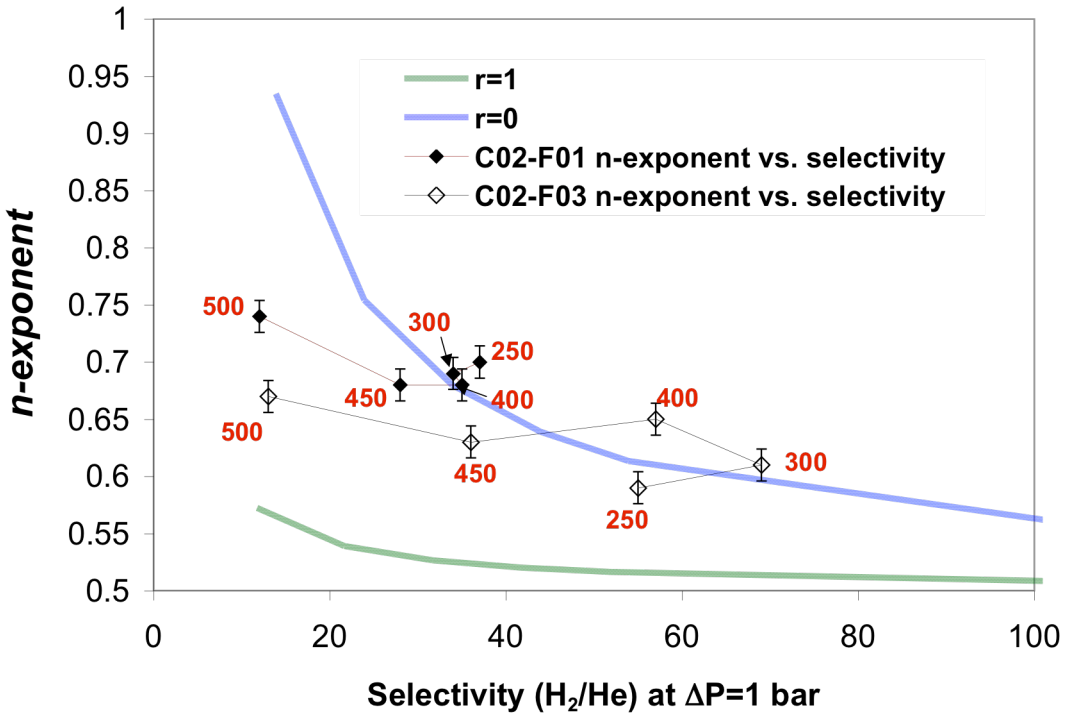

Figure 5-10 n-exponent as a function of selectivity for C02-F01 and C02-F03 membranes

Looking at the absolute values of the H_2 permeance, n-exponent and activation energy for H_2 permeation in a composite Pd membrane did not give sufficient information on the mechanism of the H_2 permeation. However, looking at the variations of the n-exponent and the variations of the activation energy for H_2 permeation with increasing temperature indicated the presence of mass transfer resistance within the support. Indeed, as temperature increases, the H_2 flux across the Pd layer increases and since the pressure drop across the porous support increases with the flux, the mass transfers resistance becomes larger at higher temperatures. Therefore, as the temperature is increased, the activation energy determined within 50ºC temperatures windows (as explained in Section 3.2.4) should decrease and the n-exponent should increase.

As an example, the H_2 permeance and E_p of membrane C01-F11b were calculated using the mass transfer model described in Section 5.2.1 with the following numerical values for LPd, $\alpha_{He}(293)$ and $\beta_{He}(293)$ that were experimentally measured.

$$L_{Pd} = 17 \cdot \mu m$$
$$\alpha(293) = 28 \cdot m^3/(m^2 \cdot h \cdot bar)$$
$$\beta(293) = 21 \cdot m^3/(m^2 \cdot h \cdot bar^2)$$

C01-F11b thickness was determined from SEM micrographs, $\alpha_{He}(293)$ and $\beta_{He}(293)$ were carefully measured after grading the support with Pd pre-activated Al_2O_3 particles. C01-F11b was a perfect example to validate the mass transfer model since no H_2 flux decline was seen at temperatures equal to or lower than 500ºC (no intermetallic diffusion). Also, leaks did not have any effect on H_2 flux since the He leak of C01-F11b at 500ºC was $2.63 \cdot 10^{-3}$ $m^3/(m^2\ h\ bar)$, which corresponded to a selectivity (H_2/He) over 400 at all temperatures.

The calculated values of $F_{0.5}$, E_p and n-exponents were compared with the experimental values obtained for C01-F11b membrane. It is important to keep in mind that none of the parameters in the model described in Section 5.2.1 were fitted to match the experimental data of membrane C01-F11b.

Figure 5-11(a) shows the experimental and predicted H_2 permeance assuming Sieverts' law ($F_{0.5}$). The model underestimated the experimental $F_{0.5}$ values by 1-2 $m^3/(m^2 h bar^{0.5})$ at all temperatures, which was due to the fact that H_2 also permeated through the grade Al_2O_3-Pd layer by the solution-diffusion mechanism. Figure 5-11(b) shows the experimental and predicted Arrhenius plots based on $F_{0.5}$. The overall activation energies within the 250-500ºC temperature range, experimental and predicted, were considered as equal with a value close to 12.5 kJ mol^{-1}. It is important to notice that the activation energy for H_2 diffusion through freestanding Pd foil was set to 14.9 kJ mol^{-1} (see Equation (4-11)) for the calculations and that the activation energy for H_2 permeation through the composite Pd membrane was calculated to be 12.7 $kJmol^{-1}$ and measured to be 12.2 kJ mol^{-1}. The difference between the predicted and measured value was within the measurement errors. Therefore, as predicted, the mass transfer resistance within the porous media led to a decrease in the activation energy for H_2 permeation. The decrease in E_p was equal to 3 kJ mol^{-1} for the particular case of C01-F11b. Figure 5-12 shows the experimental and predicted n-exponents. n-exponents are not predicted or measured to elucidate the mechanism of H_2 permeation but just as a tool to verify, how far a membrane can deviate from Sieverts' law.

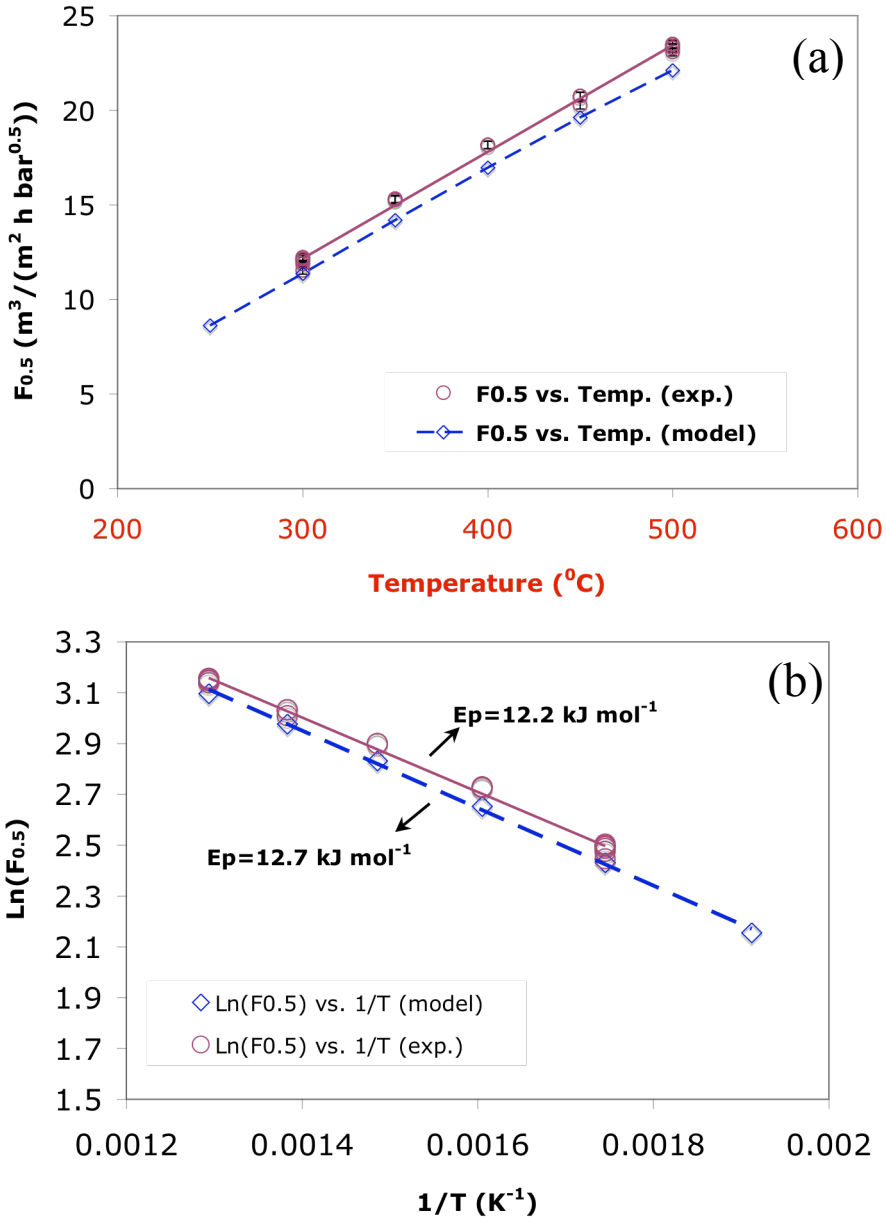

Figure 5-11 (a) Calculated and experimental H_2 permeance $F_{0.5}$. (b) Calculated and experimental activation energy based on $F_{0.5}$ values (250-500°C)

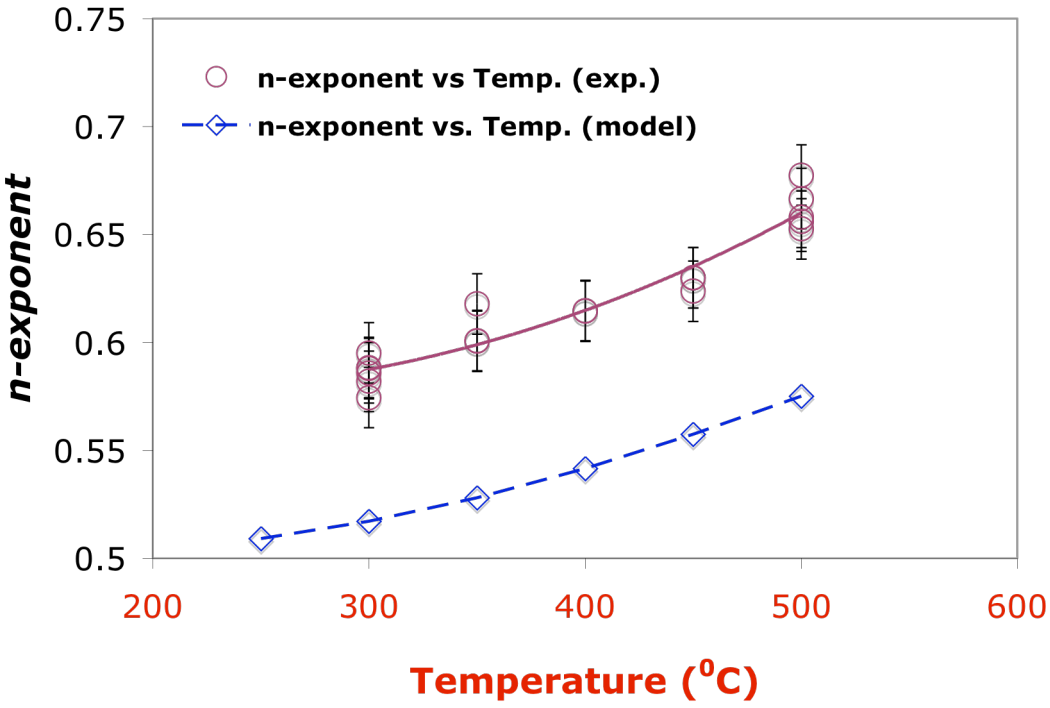

Figure 5-12 Calculated and experimental n-exponents

The model correctly predicted the trend shown by the experimental n-exponent as a function of temperature, yet, the experimental value also included other effects. That is, at higher temperatures, mass transfer resistance prevails and the n-exponent increases from 0.5 to higher values.

Figure 5-13 shows the predicted and experimental Ep for H_2 permeation values determined in small temperature intervals (250-300ºC, 300-350ºC, 350-400ºC, 400-450ºC and 450-500ºC). The E_p for H_2 differed by a maximum of 1 kJ mol^{-1} and, which is very important, in both cases the E_p decreased from a value close to 13.5 kJ mol^{-1} to a value close to 11.1 kJ mol^{-1} in agreement with the fact that at higher temperatures mass transfer within the porous support became more important. As temperature increased, the H_2 flux increased and the pressure drop across the porous support also increased, leading to higher flux resistances within the support at high temperatures.

Therefore, as already stated, the only consideration of absolute values of the H_2 permeance, activation energy and n-exponent, did not give enough information on the presence of mass transfer resistance in the porous support. However, the variations in E_p and n-exponent as temperature was increased, was a powerful indicator of the presence of mass transfer resistance in the porous support.

5.4.3.2 The prediction of mass transfer resistance in composite Pd membranes

This section aimed at the theoretical calculation of $(F_{0.5,\ foil}-F_{0.5,comp})/(F_{0.5,\ foil})$, the n-exponent and the $E_{p(450-500)}$ as a function of ξ_{250}.

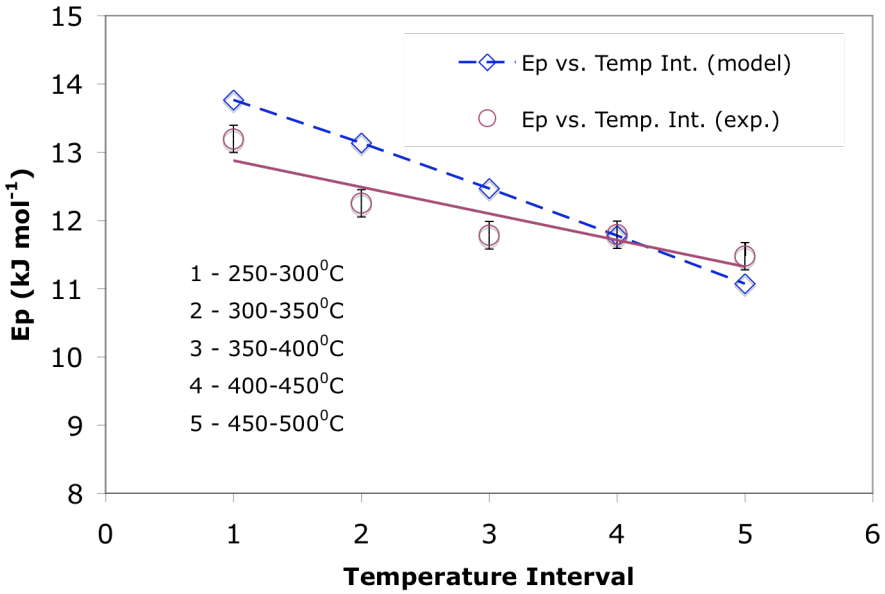

Figure 5-13 Calculated and experimental Ep changes with temperature

Having the dimensionless number ξ_{250} to compare the resistance for the H_2 flux within the Pd film and the resistance within the porous support at 250ºC under a pressure difference of 1 bar (2:1), it was possible to estimate the effect of mass transfer on the H_2 permeance, the E_p and the n-exponent for all membranes listed in Table 5-1. Table 5-1 lists the experimental He permeance parameters $\alpha_{He}(293)$ and $\beta_{He}(293)$ of the supports, the Pd thin film thickness, the determined ξ_{250} parameter and the activation energy for H_2 permeance experimentally determined in the 450-500ºC temperature interval, $E_{p(450\text{-}500)}$, for most of the membranes studied throughout this work.

The calculations were performed by setting hypothetical values of $\alpha(293)$ equal to 70 $m^3/(m^2\ h\ bar)$ and $\beta(293)$ equal to 52 $m^3/(m^2\ h\ bar^2)$ to a given porous support and decreasing the thickness of the Pd layer on that support, thereby changing the ξ_{250} parameter. The thickness of the Pd dense film, L_{Pd}, was varied between 57 and 3.8 μm so that ξ_{250} varied between 150 and 10. For each value of ξ_{250} the permeance assuming Sieverts' law, $F_{0.5}$ at 500ºC, the E_p within the 450-500ºC temperature range and the n-exponent at 500ºC were calculated using the model in Section 5.2.1 (500ºC is the temperature at which mass transfer resistance has the biggest contribution). Figure 5-14 shows the calculated n-exponents and $(F_{0.5,\ foil}\text{-}F_{0.5,comp})/(F_{0.5,\ foil})$ (percentage of the H_2 permeance of a freestanding Pd film), both at 500ºC, as a function of ξ_{250}. It is interesting to note that even for a large value of ξ_{250} (ξ_{250}>100), the composite Pd membrane only allows 93% of the freestanding Pd film H_2 permeance to pass. For ξ_{250} values higher than 100 the increase in n-exponent (0.5056) was very small.

Table 5-1 Support characteristics, Pd film thickness, ξ_{250} parameter and $Ep_{450-500}$ for all membranes in this chapter

Membrane name	Support grade (μm)	Graded	α[(a)] ($m^3/(m^2\ h\ bar)$	β[(a)] $m^3/(m^2\ h\ bar^2)$	L (Gravimetric) (μm)	L (SEM) (μm)	ξ_{250}	$Ep_{(450-500)}$ ($kJ\ mol^{-1}$)
C01-F03	0.1-PSS	No	98	73	32	37	134	n.a.[(b)]
C01-F04	0.1-PSS	No	82	62	28	Not determined	86	n. a.[(b)]
C01-F05	0.1-PSS	No	83	62	33	Not determined	102	n.a.[(b)]
C01-F07	0.1-PSS	No	100	81	23	24	92	n.a.[(b)]
C01-F08	0.1-PSS	Yes	104	84	15	19-24	58	n.a.[(b)]
C01-F11b	C01-F11	Yes	28	21	13	17	18	11.5
Ma-32	0.1 medium-PH	Yes	29	24	7.7	Not determined	8.6	9
Ma-32b	Ma-32	Yes	29	24	10	Not determined	11.2	11.7
Ma-34b	0.1 coarse-PH	Yes	9	0.6	8	9.4	2[(c)]	9.5
Ma-42	0.1 medium-PH	Yes	46	30	5.6	Not determined	9.1	9.6
Ma-45	0.1 fine-PH	Yes	78	58	9	Not determined	26	8

[(a)] The values of α and β were measured at room temperature (293K) after oxidation for non-graded supports and after the deposition of the Al_2O_3-Pd layer in the case of graded supports.

[(b)] "n. a." stands for not applicable. The H_2 permeation of membranes C01-F03/4/5/7 and /8 decreased at temperatures higher than 275-300ºC due to inter-metallic diffusion. Intermetallic diffusion led to the increase in activation energy for H_2 permeation as it will be discussed in Chapter 8. Membranes C01-F11b, Ma-32/32b/34b did not show signs of intermetallic diffusion. The selectivity (H_2/He) was also higher than 400.

[(c)] The ξ_{250} value for membrane Ma-34/34b was very low. The reason for a low ξ was due to a relatively thick Pd layer deposited during the grading process. In fact, the grade layer led to the decrease of α and β, yet the layer was permeable to H_2. Therefore, ξ should be higher than 2.

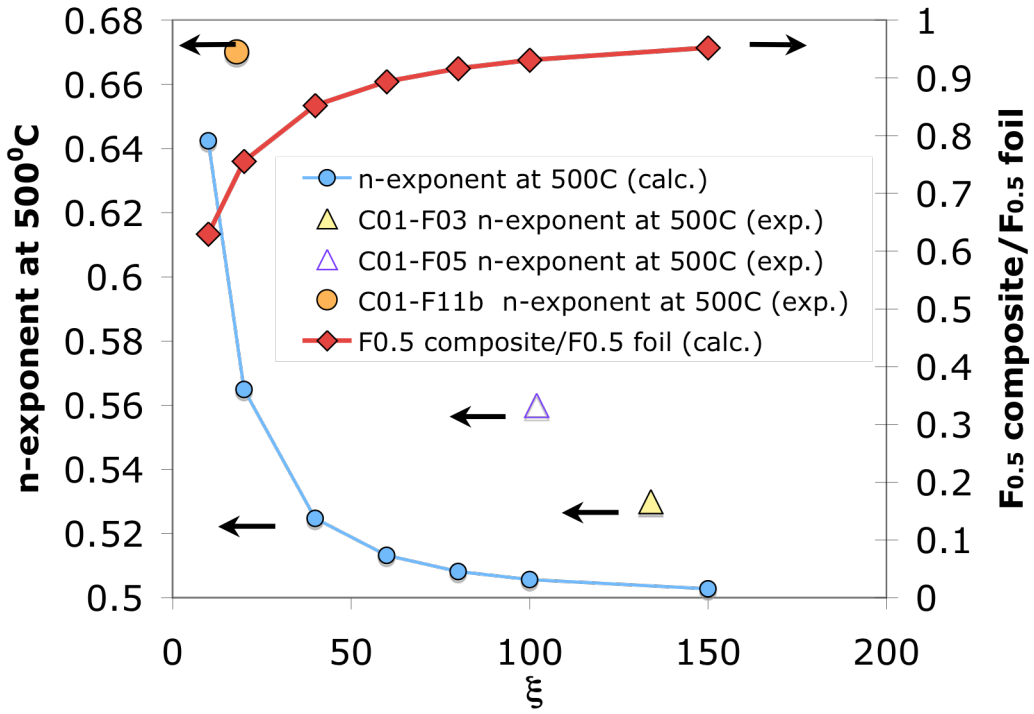

Figure 5-14 Calculated n-exponent and $F_{0.5\ composite}/F_{0.5\ foil}$ at 500°C as a function of ξ_{250}.. The experimental n-exponents determined at 500°C for membranes C01-F03/5/11b are also plotted

Therefore, mass transfer in composite Pd membranes with ξ_{250} values above 100 was negligible. The experimental n-exponents measured at 500ºC for membranes C01-F03, C01-F05 and C01-F11b also appear in Figure 5-14. As expected the experimental n-exponents measured at 500ºC increased as the ξ_{250} number decreased. Yet, the experimental n-exponents for C01-F03/5/11b were well above the n-exponents predicted by the mass transfer model indicating that experimental n-exponents were not just due to the mass transfer resistance within the support. With the ξ_{250} number being so high in the case of C01-F03/5, the mass transfer resistance within their porous support was considered as negligible. Indeed, membrane C01-F03 did not show signs of support resistance since the n-exponent at 500ºC (0.53) was close to 0.5. Moreover, the n-exponent of membrane C01-F03 decreased as the temperature was increased.

The contribution of mass transfer to the overall H_2 permeation resistance was easily detected in severe cases where the changes in the n-exponent and the changes in the activation energy for H_2 permeance as the temperature was increased were large enough to be measurable. The case of membrane C01-F11b was an ideal example since the membrane showed increasing n-exponents with temperatures and a decrease in E_p with temperature. For the cases where large variations in n-exponent and a large decrease in E_p were measured as temperature was increased, the composite Pd membrane only permeated 75% of the freestanding Pd film.

The n-exponents of membranes Ma-32, Ma-32b, Ma-34b and Ma-42 were not experimentally determined since their H_2 fluxes at high pressures were above the linearity range of the 0.3 m^3/h and/or the 1.2 m^3/h mass flow meters used. Hence, the mass transfer resistance within their support was investigated by calculating the ξ_{250} number and by considering the low activation energy for H_2 permeation measured within the 450-500ºC temperature interval. The activation energy within the 450-500ºC temperature range was determined by measuring the H_2 flux as the temperature was changed at a rate of 1ºC/min as described in Section 3.2.4. The experimental $E_{p(450-500)}$ were then compared to the $E_{p(450-500)}$ calculated by the mass transfer model of Section 5.2.1. Membranes Ma-32, Ma-32b, Ma-34b and Ma-42 were characterized by selectivities higher than 200 and did not show signs of intermetallic diffusion.

Figure 5-15 shows the calculated $E_{p(450-500)}$ as a function of ξ_{250}. The calculated $E_{p(450-500)}$ decreased as ξ_{250} decreased indicating that diffusion of H_2 through the porous media had a large contribution to the overall resistance as the He permeance of the graded support deceases and/or the thickness of the membrane becomes too thin (see Section 5.2.1). The experimental values of $E_{p(450-500)}$ measured for Ma-32, Ma-32b, Ma-34b and Ma-42 are plotted as a function of ξ_{250} in Figure 5-15.

The low activation energies for H_2 permeation measured in these membranes were in agreement with their low ξ_{250} values. Therefore, all composite Pd membranes prepared on graded PH supports were characterized by high mass transfer resistance and the H_2 permeance measured in these membranes was only equal to 60-80% of the H_2 permeance of the Pd thin film deposited on these supports.

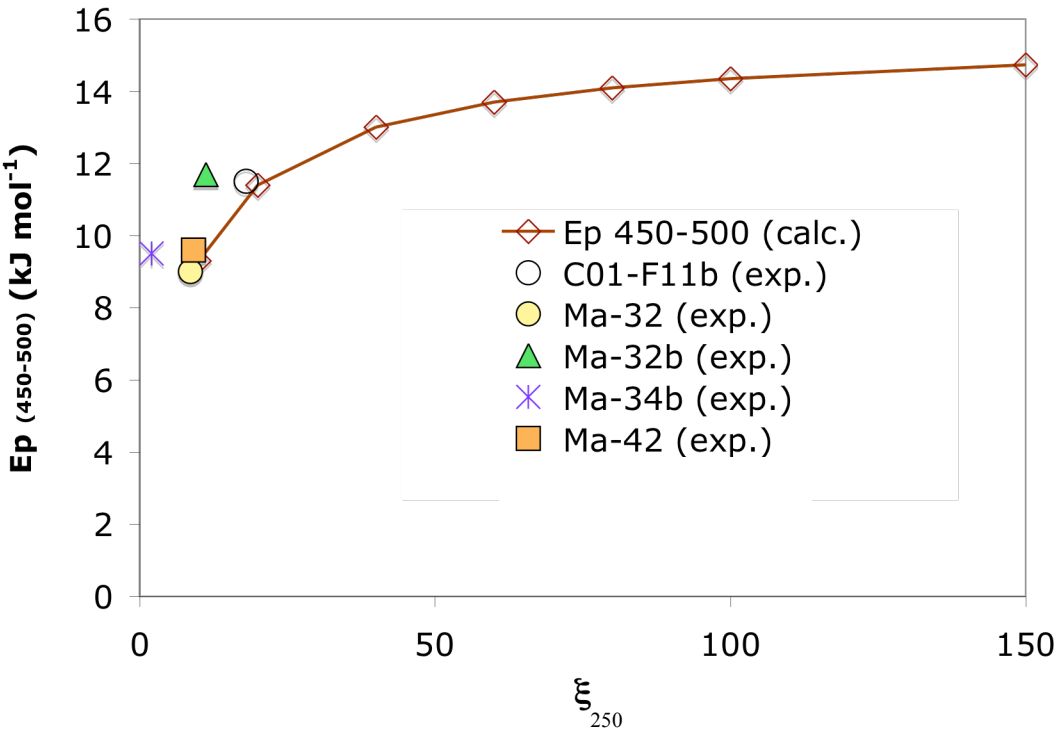

Figure 5-15 Calculated $Ep_{(450\text{-}500)}$ as a function of ξ_{250}. The experimental $Ep_{(450\text{-}500)}$ for membranes C01-F11b and Ma-32/32b/34b/42 are plotted.

5.4.4 Effect of Pd catalytic surface activity on H_2 flux

In order to accelerate the H_2 dissociation reaction on the surface of the Pd layer, C01-F05 was seeded with Pd crystallites before the H_2 characterization by Pd precipitation from a Pd plating bath containing an excess of hydrazine. The precipitated layer (light brown) was relatively thin since the shine from the underneath Pd surface was still visible. Also, the color of the membrane appeared brown due to the light scattering of small Pd crystallites on the surface. n-exponents lower than the ones shown by C01-F03 were expected. For comparison purpose, Figure 5-16 shows the n-exponent as a function of temperature for membrane C01-F03 and membrane C01-F05. Also, the n-exponents calculated from H_2 absorption isotherms (pressure effects in the 0-4.5 bar pressure range) are shown in Figure 5-16. The n-exponent from pressure effects is given by Figure 4-2 by taking the maximum pressure equal to 4.5 bar. In the temperature range 250-350ºC the n-exponents of membrane C01-F05 equaled 0.60 ±0.01 and were therefore, as expected, slightly lower than the n-exponents of membrane C01-F03 indicating a possible increase of the surface reactions rate. Surprisingly, the n-exponent of membrane C01-F05 was 0.05 units lower than the n-exponent predicted from H_2 absorption isotherms (see Figure 4-2). Above 350ºC, the n-exponents of C01-F05 membrane decreased very slowly (remained almost constant) as the temperature was increased with values similar to the n-exponents of C01-F03. Both membranes showed similar n-exponents at 500ºC (0.54 ±0.01). Therefore, Pd seeds were only effective for increasing the surface reactions rate at low temperatures. At high temperatures Pd grains in the thin Pd seeded layer increased in size leading to the loss of its catalytic activity.

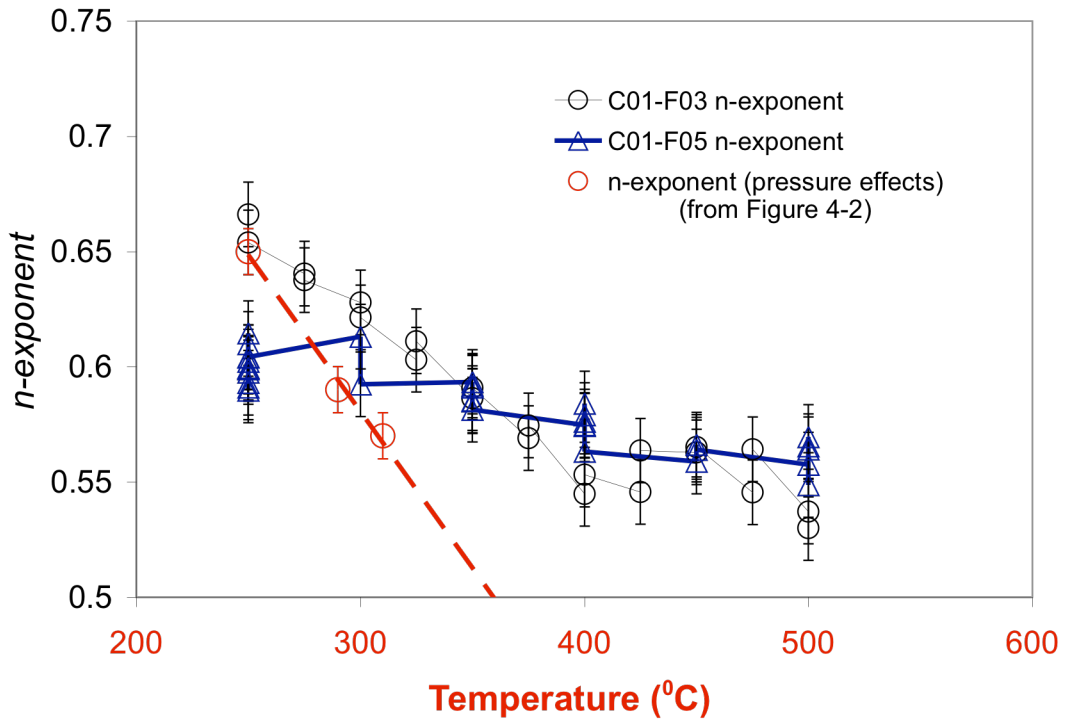

Figure 5-16 n-exponent as a function of temperature for membranes C01-F03 and C01-F05.

After the H_2 exposure at high temperatures the color of the Pd film appeared very bright indicating the growth or the sintering of Pd crystallites of the original seeded layer. Figure 5-17(a) and Figure 5-17(b) show the cross-section and the surface of membrane C01-F05, respectively. Both pictures were taken after the H_2 characterization i.e. after the exposure to H_2 at 700ºC. After H_2 exposure at 700ºC, the layer kept a very uniform thickness with a very smooth surface as shown in Figure 5-17(a). After Pd seeds sintered (T>350ºC) the surface lost its catalytic activity and membrane C01-F05 showed n-exponents similar to the n-exponents of an uncoated membrane at 500ºC, i.e. n-exponents similar to the ones shown by membrane C01-F03 in the 350-500ºC temperature range. At temperatures higher than 350ºC both membranes had similar n-exponents.

The second method used to increase the rate of H_2 dissociation on the catalytic surface of Pd was the oxidation in stagnant air at 350ºC for 48 hr, which was applied to membrane C01-F11b. The freshly prepared membrane C01-F11 was characterized at several temperatures from 250ºC to 500ºC following the same characterization procedure as C01-F03 and C01-F05. After the first characterization had been completed, the membrane was removed from the reactor, activated and Pd plated (1.5 μm) to repair the small leak that had developed during the first characterization. After the additional 1.5 μm of Pd, Pd seeds were deposited using the same procedure as on membrane C01-F05. The membrane was then oxidized in air at 350ºC for 48 hr. The surface of membrane C01-F11b after air cleaning/activation was slightly purple and not shining. Membrane C01-F11b was then characterized at temperatures ranging from 250ºC to 500ºC. The H_2 permeance based on Sieverts' driving force at 250ºC at the end of the first characterization was equal to 6.5 $m^3/(m^2\ h\ bar^{0.5})$.

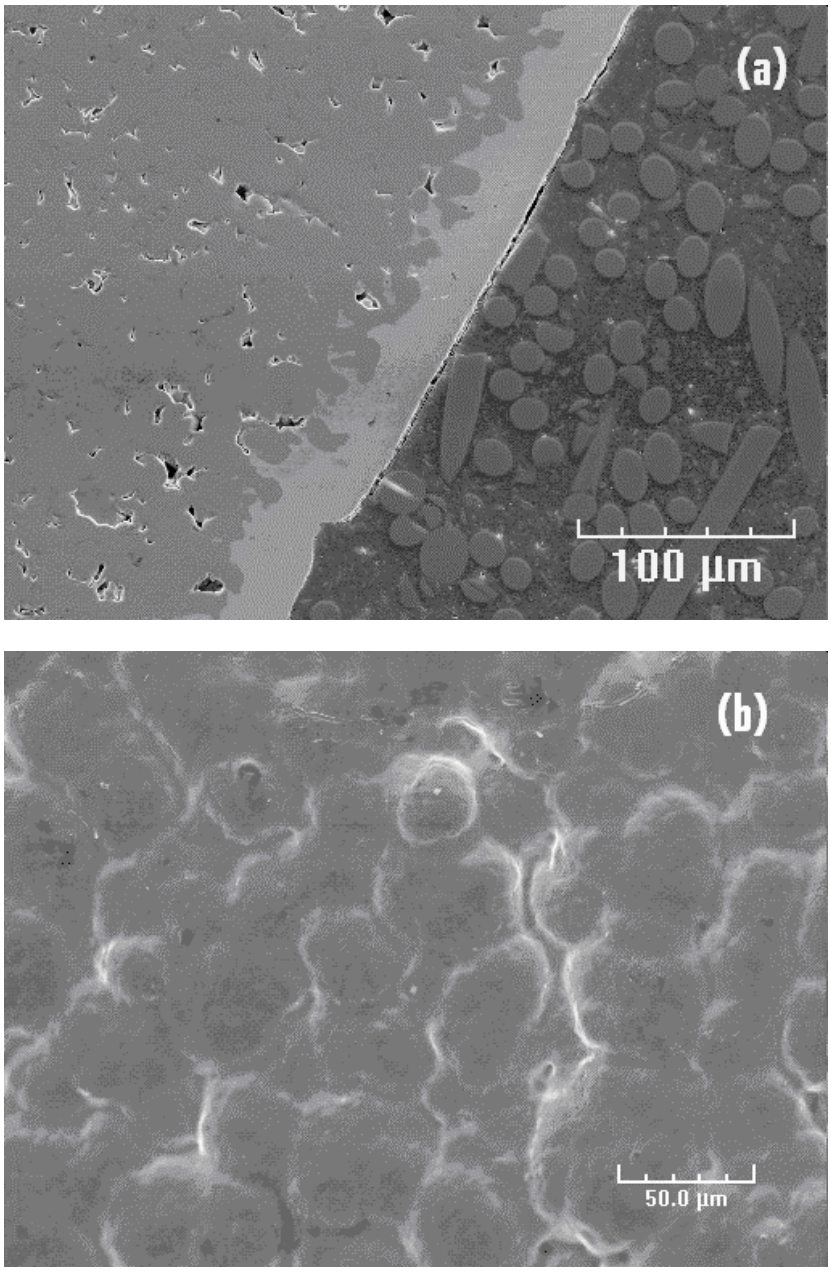

Figure 5-17 (a) Cross-section of membrane C01-F05. (b) Surface morphology of membrane C01-F05.

Even though more Pd was added on C01-F11, the H_2 permeance at 250ºC of C01-F11b equaled to 8.3 $m^3/(m^2\ h\ bar^{0.5})$ after 200 hr in H_2, which was higher than the H_2 permeance at 250ºC of C01-F11 by 1.8 $m^3/(m^2\ h\ bar^{0.5})$. Air oxidation enhanced the H_2 permeance of C01-F11. Figure 5-18(a) and Figure 5-18(b) show the cross-section and the surface morphology respectively for membrane C01-F11b after the H_2 characterization. The oxidation in air led to the formation of hills and valleys, encircled in Figure 5-18(a) and seen from the top in Figure 5-18(b), similar to the ones reported in the literature (Aggarwal et al., 2000; Roa et al., 2003). The formation of hills and valleys resulted in a composite Pd membrane with higher H_2 flux than the initial composite Pd membrane. It was also possible that air oxidation/H_2 reduction led to the formation of porous Pd layer, which increased the H solubility at the surface (Radzhabov et al., 1980; Roshan et al., 1983).

During the characterization of C01-F11 the n-exponents ranged between 0.64 and 0.68 over the entire studied temperature range (300ºC-500ºC) as shown in Figure 5-19. After Pd plating and surface reactivation, the n-exponent of C01-F11b was equal to 0.58 at 250ºC similar to the n-exponent shown by membrane C01-F05 at 250ºC. Hence, the n-exponent of membrane C01-F11b at 250ºC was also lower than the n-exponent predicted by the 250ºC H_2 absorption isotherm. As already shown, the n-exponents of membrane C01-F011b increased from 0.58 at 250ºC up to 0.66 at 500ºC with a similar trend as the one predicted by the mass transfer model. The n-exponents predicted by the mass transfer model were also plotted as a function of temperature in Figure 5-19 with 0.09 units added to all n-exponents calculated in order to fit the calculated and the experimental n-exponent at 250ºC.

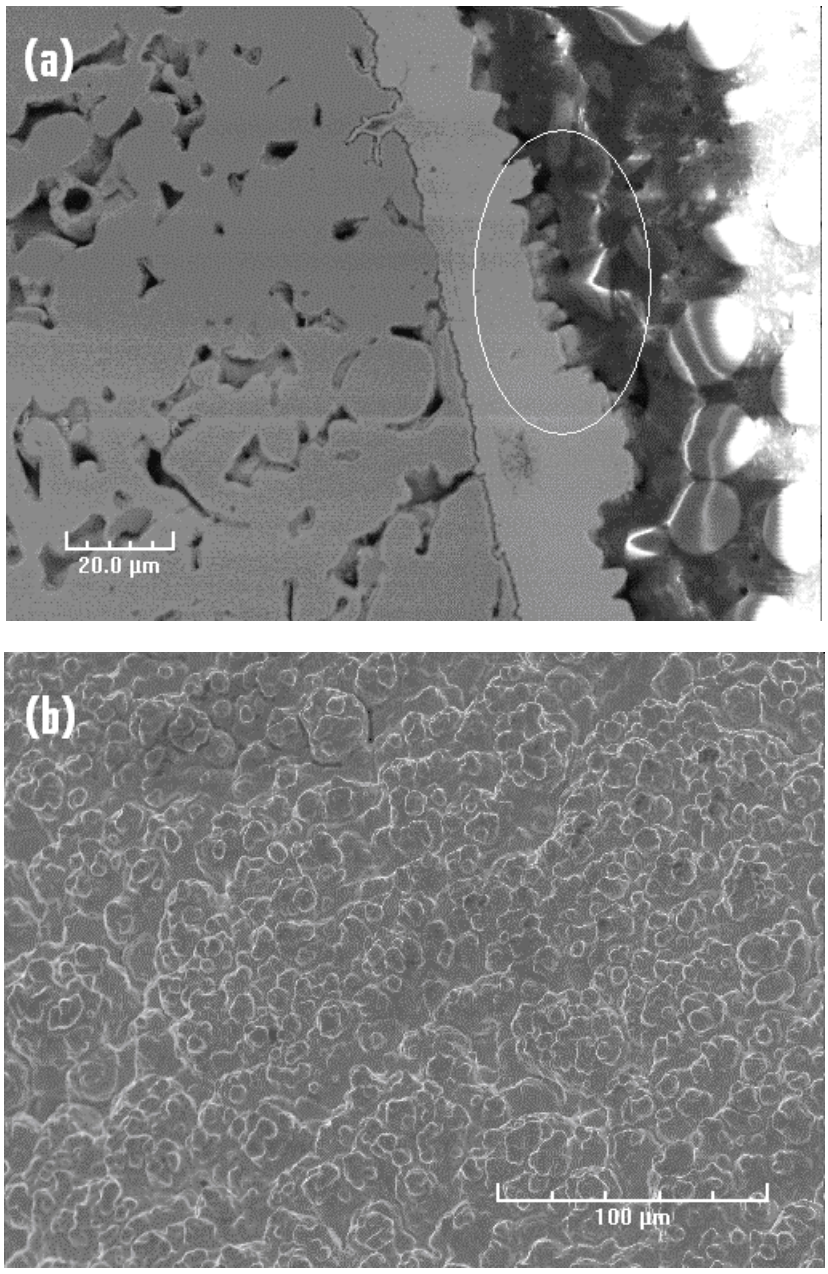

Figure 5-18 Cross-section (a) and surface analysis (b) of membrane C01-F11 after H_2 characterization.

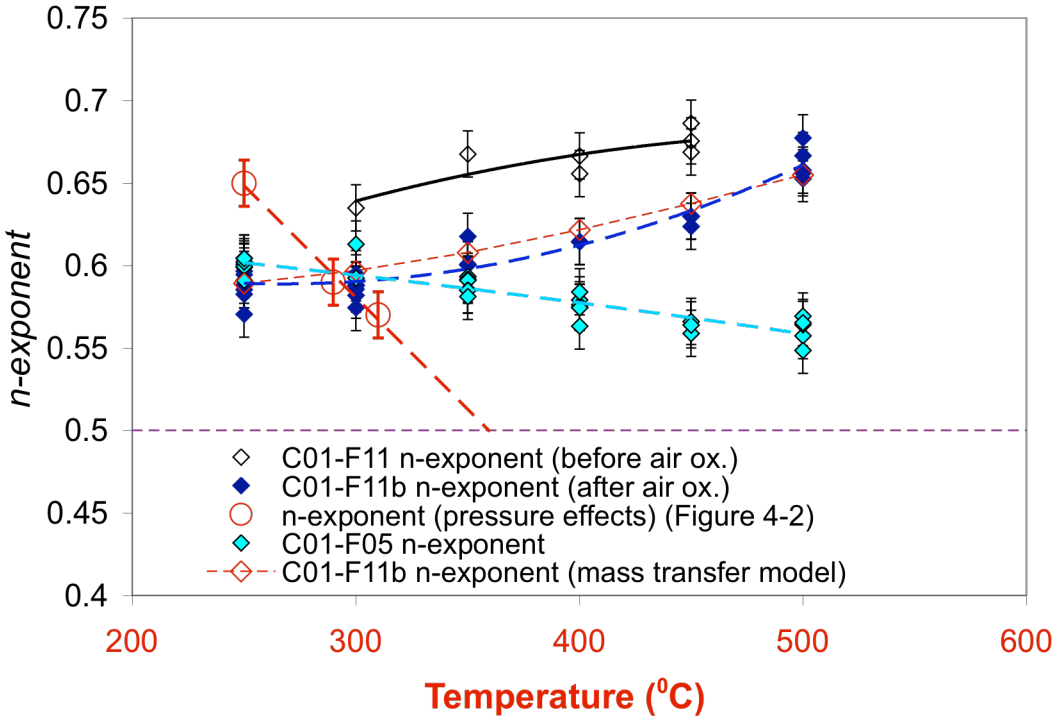

Figure 5-19 n-exponent as a function of temperature for membranes C01-F05, C01-F11a and C01-F11b. n-exponents due to pressure effects and the calculated n-exponents for C01-F11b due to mass transfer effect (Figure 5-12) were also added for comparison purposes.

A change in membrane color was also noticed for membrane C01-F11b after exposure to high temperatures in H_2 atmosphere. The surface of the membrane changed from purple after oxidation to silver color (Pd color) with little shine. A deactivation of the surface similar to C01-F05 membrane occurred. At 300-350ºC and higher temperatures Pd grains included in the spongy catalytic layer grew and lost their H_2 dissociative capabilities. Reactivation by surface oxidation at 350ºC also increased the reactions rate at the surface since the n-exponents shown by membrane C01-F11b were lower than n-exponents shown by C01-F11

Membranes C01-F05, C01-F11 and C01-F11b clearly showed that Pd seeding and air cleaning/oxidation increased the surface reaction rate. Therefore, even if the bulk diffusion was the main resistance for H_2 permeation, surface reaction resistances still contribute, though in a reduced extent, to the transport of H_2. Surface reactions even had a more pronounced resistance at lower temperatures mainly due to the presence of impurities adsorbed on the Pd surface. Impurities were removed by heating (n-exponent decreasing with temperature) and air oxidation at 300-350ºC.

5.4.5 The activation energy for H_2 permeation in fresh composite Pd membranes

5.4.5.1 The Ep in fresh composite Pd membranes

As already stated in Section 3.2.4, the activation energy for H_2 permeation was measured by using two different methods: (1) considering steady state permeance values, $F_{0.5}$, after the membranes spent a long time at a given temperature and (2) measuring the H_2 flux at a ΔP of 1 bar (2:1) while changing the temperature at a rate of 1ºC/min. The two

methods did not lead to the same numerical value of the activation energy in fresh composite Pd membranes. Indeed, all composite Pd membranes had a different H_2 permeance vs. time response. The H_2 permeance can increase as a function of time due to an increase of leaks, contaminants desorption from the surface and "rearrangements" (mostly seen in composite Pd membranes prepared on graded supports). In addition, the H_2 permeance can increase during alloying of Pd-Cu layers. The H_2 permeance can also decrease as a function of time, which is generally attributed to intermetallic diffusion. The objective of the following section was to demonstrate that using method (1) to determine E_p in a fresh membrane led to erroneous values of E_p. Also, that method (2) is more suitable for fresh composite Pd membranes.

Figure 5-20 shows the H_2 permeance, F_{H2}, of C01-F03 membrane as a function of time at different temperatures. The dashed lines represent the 50ºC temperature changes. At each temperature F_{H2} decreased due to intermetallic diffusion. Figure 5-21 shows the Arrhenius plot of $F_{0.5}$ permeance values determined twice at each temperature (see Section 3.2.3 to recall the difference between F_{H2} and $F_{0.5}$). The "saw" shape in Figure 5-21 is due to the fact that between each determination of $F_{0.5}$ the permeance decreased due to intermetallic diffusion. Hence, the determination of the activation energy for H_2 permeance based on $F_{0.5}$ values would be impossible in this case. Fitting a straight line to the experimental data of Figure 5-21 would lead to a negative value of E_p. In order to determine the activation energy for H_2 permeation the H_2 flux, J_{H2}, between each temperature change had to be considered.

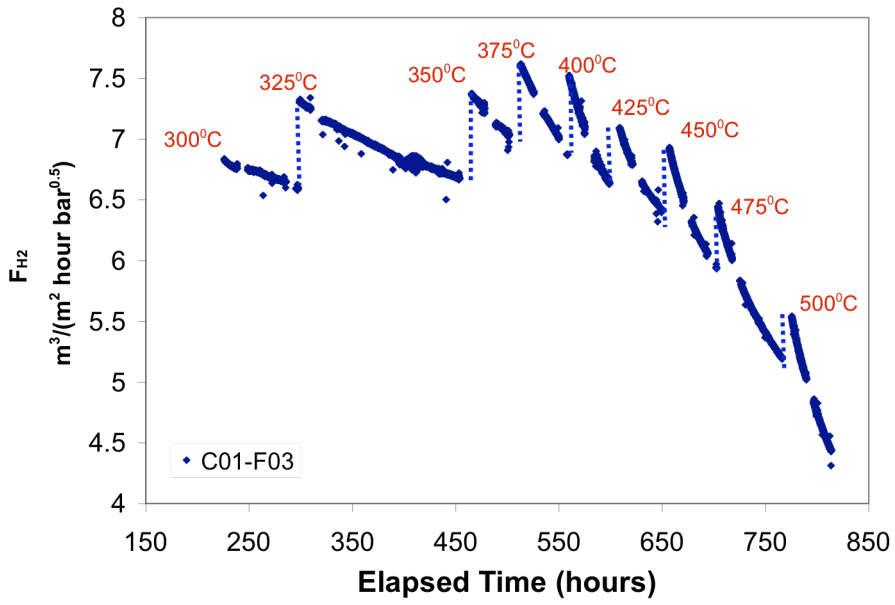

Figure 5-20 F_{H2} permeance as a function of time at different temperatures C01-F03

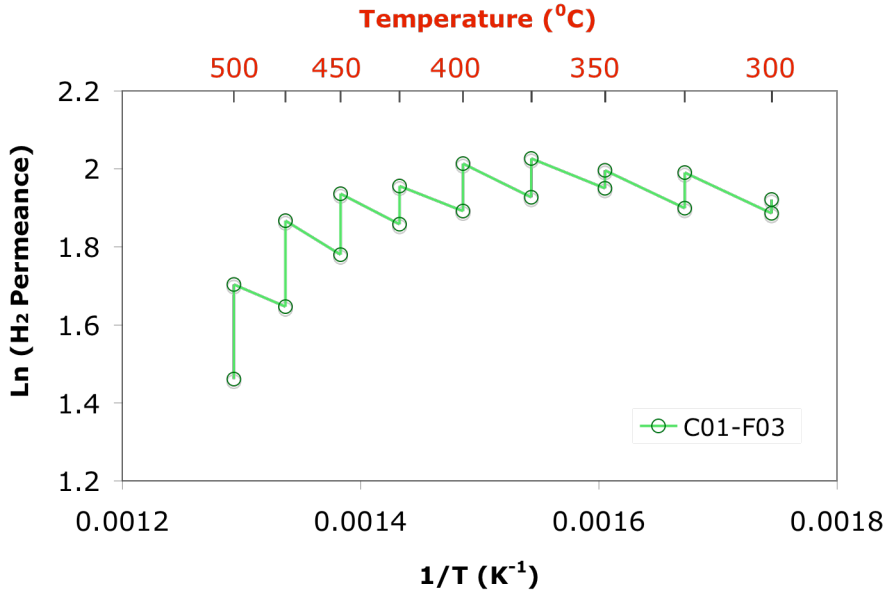

Figure 5-21 $Ln(F_{0.5})$ as a function of 1/T for membrane C01-F03

The determination of the activation energy from H_2 permeance from experimental data taken during temperature change at 1ºC/min leads to a better estimation yet, the following important condition needs to be fulfilled. Figure 5-22 shows the H_2 permeance and temperature as a function of time during the 300-350ºC temperature change for membrane Ma-41. Δ1 is the increase in permeance due to the 50ºC increase in temperature, Δ2 is the increase in permeance (due to any process leading to permeance increase in green membranes over time) during the next 50 minutes after the temperature change and Δ3 is the total increase in permeance after 50-100 hr. Considering H_2 data during the temperature change is only valid if the increase of permeance (due to processes affecting permeance over long periods of time) during the 50 minutes of the temperature change is negligible to the increase of H_2 permeance due to temperature. That is, the E_p from temperature change is accurate if $\Delta 2 << \Delta 1$.

Figure 5-23 shows the H_2 permeance, F_{H2}, as a function of time for the 250-300ºC temperature change for membrane Ma-41. This Figure shows that at this particular temperature change, Δ2 is not negligible compared to Δ1. The particular case of Figure 5-23 was due to the alloying of the Pd-Cu bi-layer. Composite pure Pd membranes showed a similar behavior at 250ºC, especially green membranes prepared on graded supports with pre-activated powder. However, for all membranes, the condition $\Delta 2 << \Delta 1$ was fulfilled for the 300-350, 350-400, 400-450, 450-500ºC temperature changes.

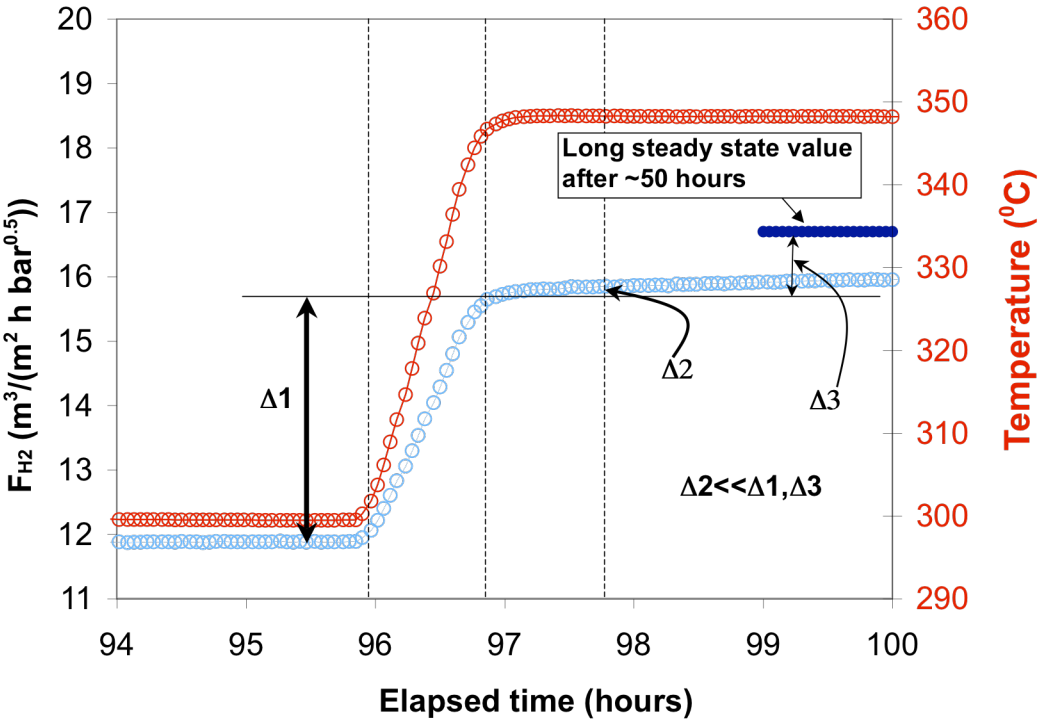

Figure 5-22 Temperature change between 300 and 350ºC of membrane Ma-41

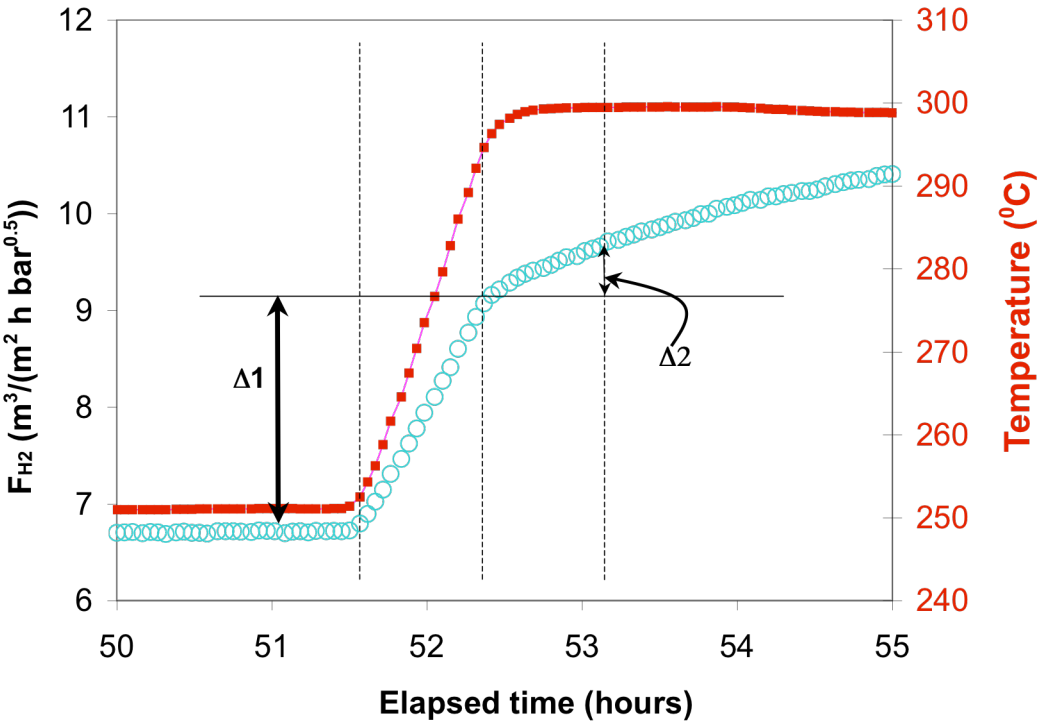

Figure 5-23 H_2 permeance, F_{H2}, as a function of time during the 250-300ºC temperature change in Ma-41

Figure 5-24 shows the activation energy determined in the 300°C-400°C temperature range of membrane C02-F01 by the two methods: based on long time steady states values and steady state values while changing the temperature. The discontinuity in the $Ln(F_{0.5})$ vs. 1/T function between points (b) and (c) and points (d) and (e) in Figure 5-24 are due to the growth of leaks (defects) during the time the membrane was held at 350°C and 400°C. The selectivity (H_2/He) of C02-F01 at 300, 350 and 400ºC was only around 30. The activation energy in the 300°C-350°C temperature range and in the 350°C-400°C temperature range determined while changing temperature were equal to 10.1 kJ mol^{-1} and 10.6 kJ mol^{-1} respectively and the overall activation energy estimated from $F_{0.5}$ values was equal to 14.2 $kJmol^{-1}$. Since defects formation results in an increase of the portion of the H_2 that flows by slip flow diffusion (Knudsen + viscous), the activation energy for H_2 permeance should decrease according to the activation energy of gas diffusion. Therefore, the H_2 permeance of a composite Pd membrane with low selectivity should have a lower activation energy than 14.9 kJ/mol (see Equation (4-11)). Activation energy values of 10.1-10.6 kJ mol-1 are then consistent with the low selectivity of C02-F01 membrane and the activation energy based on steady state values after long times (14.2 kJ/mol) has no real meaning.

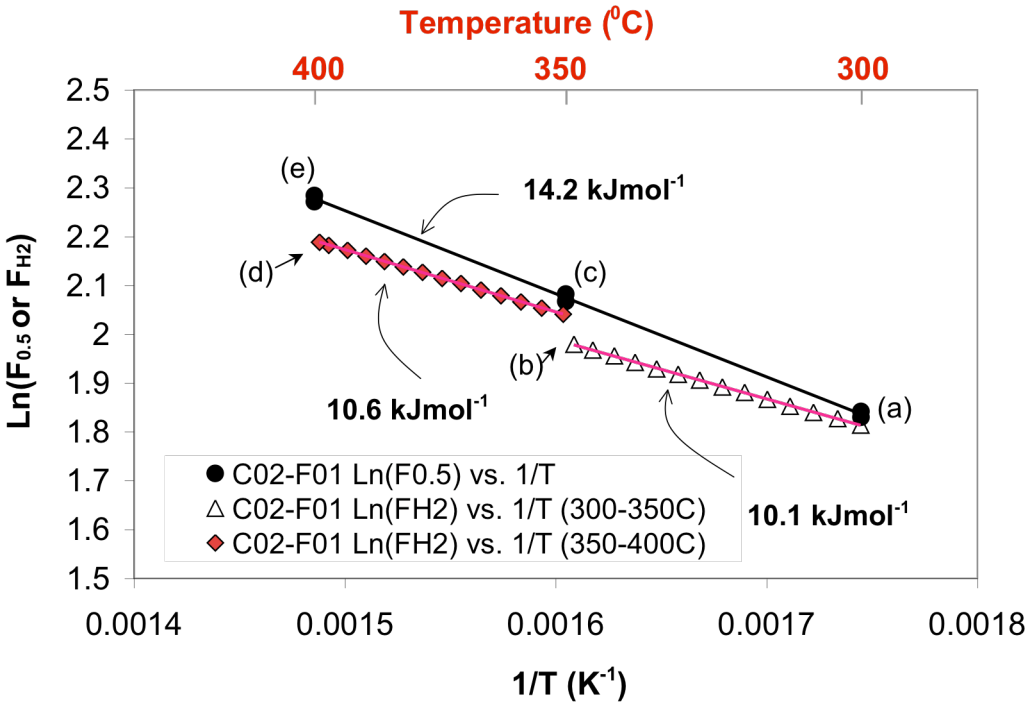

Figure 5-24 Ln($F_{0.5}$) and Ln(F_{H2}) vs. 1/T for membranes C02-F01.

Also, both methods (E_p based on $F_{0.5}$ H_2 permeance values and E_p based on F_{H2} H_2 permeance while changing the temperature) gave the same value for the activation energy of H_2 permeance in stable membranes, i.e. when no H_2 flux increase or decline is seen and when the membrane is perfectly dense. As example, the activation energy for H_2 permeation of membrane C01-F05 was determined by the two methods in the 250°C-350°C temperature range and the Arrhenius plot is shown in Figure 5-25. C01-F05 showed selectivities (H_2/He) over a 1000 at all temperatures.

The activation energy in the 250°C-300°C temperature range and in the 300°C-350°C temperature range determined while changing temperature were equal to 10.4 kJ mol^{-1} and 10.9 kJ mol^{-1} respectively. The overall activation energy estimated from $F_{0.5}$ H_2 permeance values was equal to 10.2 $kJmol^{-1}$.

Hence, considering F_{H2} when the temperature was changed at rates equal to or slower than 1°C/min led to a better determination of the activation energy for H_2 permeation. It has to be noted that the activation energy from method (1) and (2), if they did differ, they differed the first time the membrane was characterized at high temperatures. Indeed, once a membrane was exposed to the highest temperature (500ºC or higher), determining again the activation energy for all 250-300, 300-350, 350-400, 400-450 and 450-500ºC temperature intervals would give exactly the same value and, furthermore, a value equal to the E_p considering long term $F_{0.5}$ H_2 permeance. That was due to the fact that, during the second characterization, membranes did not undergo processes that would either lead to the decrease or the increase of the H_2 flux as a function of time.

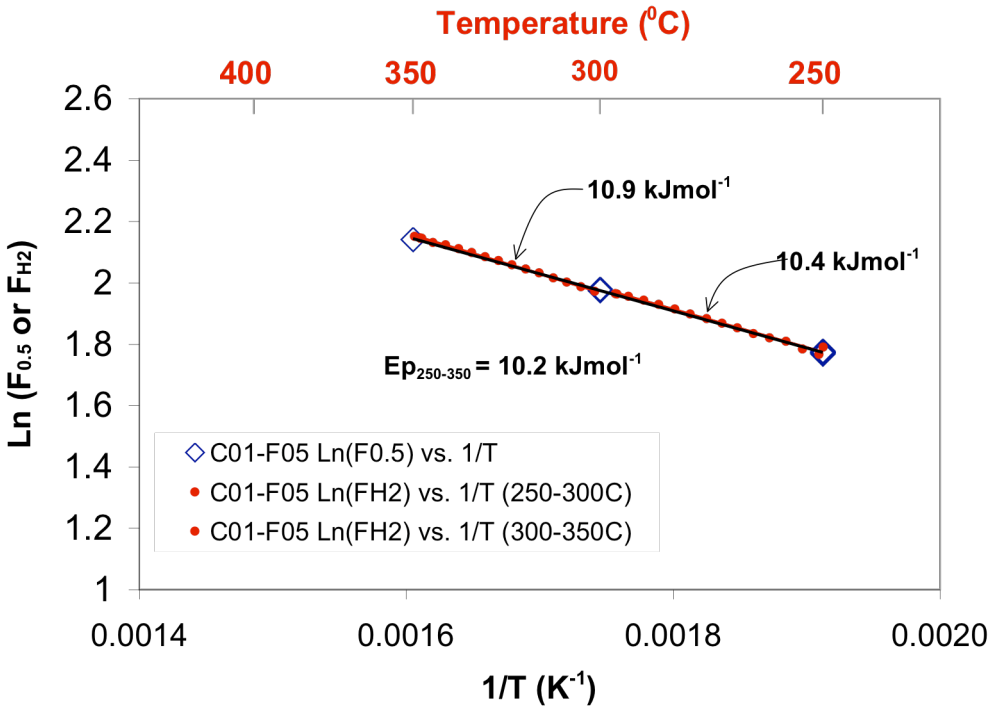

Figure 5-25 $Ln(F_{0.5})$ and $Ln(F_{H2})$ vs. 1/T for membranes C01-F05.

The determination of the E_p based on data taken during temperature change gave valuable information on the state and the H_2 permeation mechanism of the membrane at that particular moment. Therefore, it was possible to elucidate the processes taking place within the membrane as the temperature was increased. For instance, the E_p based on data taken during temperature changes decreased as higher temperature intervals were considered (300-350ºC -> 450-500º) if leaks appeared and grew. Also, a decrease in activation energy was explained by an increase of the support resistance contribution to the overall H_2 permeation resistance at high temperatures. On the contrary, an increase in activation energy was explained by intermetallic diffusion, which will be discussed in Section 8.3.2.

5.4.5.2 Activation energy measured at low temperatures in composite Pd membranes

From a fundamental point of view, it is very important to characterize the H_2 permeation properties of composite Pd membranes at low temperatures. At low temperatures, 250-300ºC, the microstructure of the electroless deposited Pd films was considered as "fresh" since no significant changes occurred (see Chapter 9, Figure 9-4). Table 5-2 lists the activation energy for the H_2 permeation determined by measuring H_2 flux as the temperature was increased for the 250-300ºC temperature range ($E_{p(250-300)}$) and the 300-350ºC temperature range ($E_{p(300-350)}$) for membranes C01-F03/5/7/8/11/11b. The activation energy for H_2 permeation of a fresh membrane, having a fine-grained structure, was found to be relatively low 9-12 kJ mol^{-1} in the 250-300ºC temperature range compared to the activation energy for H_2 permeance reported in the literature 13-19 kJ mol^{-1} (see Section 4.2.3). The low activation energy could not be explained by leaks since the He leak of all membranes was undetectable at such low temperatures. In addition, mass transfer

resistance at low temperature for membranes C01-F03/5/7/8/11/11b was negligible. It is believed that the reason for the low activation energy for H_2 permeance found in electroless deposited composite Pd membranes at low temperatures was due to the fine-grain structure that characterizes these membranes.

Table 5-2 $Ep_{(250-300)}$ and $Ep_{(300-350)}$ for C01-F03/5/7/8/11/11b membranes

Membrane	E_p (0.5) ±0.2 (250-300ºC)	E_p (0.5) ±0.2 (300-350ºC)
C01-F03	12.0	12.7
C01-F05	10.4	10.9
C01-F07	9.8	10.6
C01-F08	10.4	11.8
C01-F11	9.4	11.24
C01-F11b	10.3	12.3

Indeed, in a polycrystalline sample H_2 can diffuse along the boundaries between Pd crystallites i.e. grain boundaries. The diffusion through grain boundaries is characterized by an activation energy, which is believed to be lower than that of 'bulk diffusion' (Porter and Easterling, 1981). That is, at low temperatures, H_2 would essentially diffuse through grain boundaries in a polycrystalline Pd layer. At higher temperatures, both 'bulk diffusion' and grain boundary diffusion would occur and it is believed that the diffusion through the grain boundaries would still be faster than 'bulk diffusion'. However, grain boundaries represent a small fraction of the total diffusion sites, which are the sum of interstitial sites and grain boundaries sites. Therefore, more H_2 would diffuse through the bulk than through grain boundaries at high temperatures even though diffusion through 'narrow pathways' (the grain boundaries) is faster than 'bulk diffusion'.

5.5 Conclusions

The H_2 permeance of composite Pd membranes was determined using two methods: assuming Sieverts' law (n=0.5) and performing a non-linear regression on the experimental data to determine the n-exponent and the permeance. The n-exponent of a fresh composite Pd membrane (with no surface modification) decreased from 0.67 to 0.53 as temperature was raised from 300 to 500ºC mainly due to the fact that at higher temperatures the relation $P^{0.5}$ vs. n(H/Pd) could be considered as linear in the 0-4.5 bar pressure range (reduction of pressure effects). Also the n-value decreased due to the removal of contaminants. The activation of the surface by Pd seeding or air oxidation at T>300ºC slightly increased the rate of H_2 adsorption/desorption reactions. Air oxidation enhanced the H_2 permeance of membrane C01-F11b. The activity of the freshly formed Pd activated surface decreased due to Pd crystallites sintering at high temperatures. It was computed and validated that H_2 leaks through defects had no contribution to the n-exponent if the selectivities were over 200-300. Adjusting the n-exponent led to better fits of the H_2 flux than assuming Sieverts' law although it is important to understand that F_n and the n-exponent cannot be used to compare membranes. The n-exponent was used as a tool to assess the presence of large mass transfer resistance or large leaks although the right H_2 permeance value to report is $F_{0.5}$. The activation energy for H_2 permeation determined by the measurement of the H_2 flux, J_{H2}, while changing the temperature at a rate of 1ºC/min appeared to be accurate and a good method for the elucidation of the H_2 permeation mechanism or the internal modifications undergone by the composite Pd membranes as temperature was increased. It also appeared, that all fresh composite Pd membranes have a relatively low E_p, which was attributed to the fine grain structure.